Geophys. J. Int. (1993) **115**, 799–818

Microearthquake seismicity and fault-plane solutions in the southern Aegean and its geodynamic implications

Denis Hatzfeld,[1] Marc Besnard,[1] K. Makropoulos[2] and P. Hatzidimitriou[3]

[1] *Laboratoire de Géophysique Interne et Tectonophysique, Observatoire de Grenoble, IRIGM. BP 53 X, 38041 Grenoble Cedex, France*
[2] *Department of Geophysics, University of Athens, 15784 Ilissia, Athens, Greece*
[3] *Seismological Laboratory, Aristotelian University, PO Box 352-1, 54006 Thessaloniki, Greece*

Accepted 1993 April 19. Received 1993 April 19; in original form 1992 June 15

SUMMARY

Seismicity ($Ml < 3.5$) in the southern Aegean, located using data collected during seven weeks of recording by a temporary network of seismological stations, largely follows the Hellenic arc; the Sea of Crete is nearly aseismic, and only little activity is located south of the Hellenic trench, within the African plate. Focal mechanisms exhibit reverse faulting in the external part of the arc and normal faulting inside it. This normal faulting indicates N–S extension in the northern Aegean, the Gulf of Corinth, the Cyclades and Dodecanese Islands, but NW–SE extension in southern Peloponnese and western Crete and E–W extension in eastern Crete. This non-uniform strain pattern suggests that the Aegean region not only extends in a N–S sense, with the Hellenic arc moving south-westward relative to the Eurasian plate, but also by E–W extension of its southern margin, so that there is a net divergence of material.

Key words: Aegean, fault plane solutions, microseismicity.

INTRODUCTION

The Aegean is a region of inhomogeneous deformation between the African and the European lithospheric plates which are converging at about 1 cm yr^{-1} with a N–S orientation (Argus *et al.* 1989). The relative motion of the Aegean arc relative to Africa, however, is thought to be much more rapid, at a rate of 7–10 cm yr^{-1}, and with a south-west direction (McKenzie 1972; Le Pichon & Angelier 1979). This rapid motion is responsible for active northward subduction of the African plate beneath Aegea and for a downgoing slab that is not parallel to the Hellenic trench. In the West, the slab dips gently beneath Peloponnese and then steepens 200 km from the trench, but the slab beneath the Sea of Crete is steeper (Hatzfeld *et al.* 1993). In addition, the Aegean region itself has undergone intense and rapid deformation since Pliocene times (Angelier 1979; Mercier 1981). The present deformation, inferred from tectonic observations, is not uniformly distributed within the Aegean region: thrust faulting is observed in Corfu and the Ionian Islands, with compression mostly perpendicular to the trench; normal faulting and N–S extension are observed in the islands of the North Aegean Sea and in the Gulf of Corinth; E–W extension is observed in southern Peloponnese and in the Dodecanese Islands (Mercier 1981; Angelier *et al.* 1982). In Crete, extension trends E–W in the West, but NE–SW in the central area, and NNW–SSE in the East (Angelier 1979). These observations are based on fault scarps, and therefore only in continental Greece and the islands.

Palaeomagnetic results (Laj *et al.* 1982; Kissel, Laj & Mazaud 1986; Kissel & Laj 1988) suggest that Peloponnese has rotated 25° clockwise since Miocene time, and that parts of western Turkey have rotated 30° counter-clockwise. Apparently Crete and the Dodecanese Islands have not rotated since that time. Recently, GPS geodetic measurements conducted around Peloponnese and Evvia (Billiris *et al.* 1991) confirm the existence of important internal deformation, and slight rotation.

Another tool that can be used to study active deformation is the seismicity, including focal mechanisms. There are, however, several limitations to the information provided by earthquakes. First, deformation is revealed only in the upper brittle part of the lithosphere. According to Jackson & McKenzie (1988), in the northern Aegean most of the extensional deformation in the brittle upper crust occurs seismically but this is not the case for the shortening in the Hellenic arc where only 15 per cent of the deformation is apparently seismic. Second, the duration for which we have precise and quantitative seismological information is very short and may not reveal the true magnitude of the strain rates even if the orientation of the principal horizontal strain rates can be estimated (e.g. Ekström & England 1989).

In the Aegean, earthquakes can be located to within about 20 km using teleseismic arrival times when their magnitudes are large enough (>4.0) to be recorded by a sufficient number of stations without an important azimuthal gap. Errors in focal depth are likely to be greater unless recordings by local stations or of *pP* phases are available (Hatzfeld & Martin 1992). Because the seismicity in the Aegean is of moderate level (there are only about 100 earthquakes yr^{-1} with $M > 4.0$), the number of reliably located events is rather small. The regional seismological network is neither very dense (the mean spacing between stations is of about 200 km except in Chalkidiki) nor very sensitive, especially for stations located on islands in the Aegean Sea (because of the microseismic noise), and so the control in the location, and especially in the depth, of the earthquakes is not very good.

Most of the reliable focal mechanisms, in the Aegean, have been determined using polarities recorded by the long-period stations of the World Wide Standard Seismological Network (McKenzie 1972, 1978; Anderson & Jackson 1987) or body wave modelling (Taymaz, Jackson & Westaway 1990; Taymaz, Jackson & McKenzie 1991; Kitatzi & Langston, 1989, 1991; Kiratzi, Wagner & Langston 1991). Mechanisms using the relative amplitude method (Liakopoulou, Pearce & Main 1991) or the centroid-moment tensor (Ekström & England 1989) have also been computed for this region. Most of the focal mechanisms are for earthquakes of relatively large magnitude and are therefore located either along the Hellenic trench, or in the northern Aegean Sea. A few tens of reliable focal mechanisms are available for these areas, but for the regions located just north of the Hellenic trench, almost no solutions are available, and it is not possible to infer, from teleseismically computed mechanisms, a continuous strain pattern for the whole Aegean region.

DATA

During the summer of 1988 a network of 82 portable seismological stations was installed over the islands of the southern Aegean Sea and Peloponnese (Fig. 1). Most of the instruments were smoked paper recorders (Sprengnether MEQ-800) connected to a 1 Hz seismometer. The stations were visited every 2 days for maintenance and to check the internal time against an external radio time. More details about the network and the instruments can be found in Besnard (1991) or in Hatzfeld *et al.* (1993).

In this paper we will not describe the numerous tests that we usually conduct to search for the most probable velocity

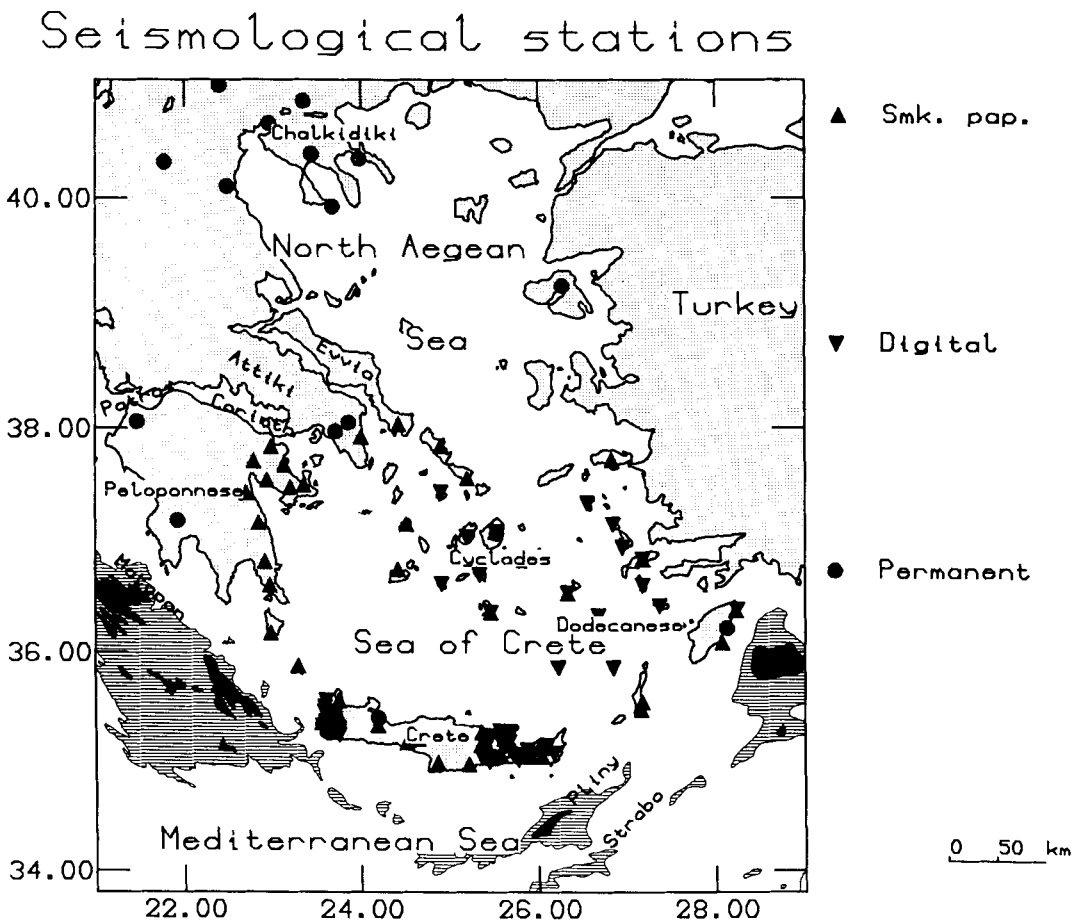

Figure 1. Map of the temporary network that was installed during the summer of 1988. The bathymetry is shown by 3000 m and 4000 m contours.

structure and to evaluate the uncertainties in the location of the earthquakes. Details about the procedures can be found in Chatelain *et al.* (1980), Ouyed *et al.* (1983), Grange *et al.* (1984), Hatzfeld *et al.* (1989, 1993), and Besnard (1991). These tests are conducted to determine which events have locations with uncertainties less than a certain value (10 or 20 km) and to eliminate all the poorly located events.

Among the 828 events that we recorded during the seven weeks of the experiment, we kept only the 766 events whose locations are constrained by at least 8*P* and 1*S* arrival times; 417 of these events were earthquakes with uncertainties smaller than 20 km, and of these 148 were with uncertainties smaller than 10 km. In this paper we will consider only the 688 crustal events located shallower than 40 km. Among them, 381 were located with uncertainties smaller than 20 km, and of these 127 were events with uncertainties smaller than 10 km.

We computed focal mechanisms using a minimum of 8 *P*-wave polarities on the focal sphere. We took into consideration the quality of the polarity readings, the type of wave (direct or refracted), and the azimuthal coverage on the focal sphere in order to separate the solutions into three categories of reliability. In category 1 we have the mechanisms for which the two planes are constrained within 20°. In category 2 only one plane is well constrained, but the *P* and *T* axes are determined within 20°. In category 3 neither of the planes are constrained with 20°, and we can use these solutions only to give an indication of the type of faulting (normal or reverse).

We also computed mechanisms using the computer program designed by Reasenberg & Oppenheimer (1985). This program provides uncertainties for the focal mechanism solutions based on the consistency of the polarities, but not on the quality of the readings. The uncertainty in the mechanism is mostly a function of the distribution of polarities on the focal sphere. We used both methods to separate the three categories.

RESULTS

Figure 2 shows a seismicity map of the 688 earthquakes shallower than 40 km, and Fig. 3 shows the 381 earthquakes that are located with uncertainties smaller than 20 km. most of these earthquakes occurred along the Hellenic arc, just behind the trench, outside of the network. No event was reliably located south of the axis of the Hellenic trench at a distance greater than 50 km, and very little activity was observed within the Sea of Crete. During our investigation we recorded a few earthquakes of magnitude larger than

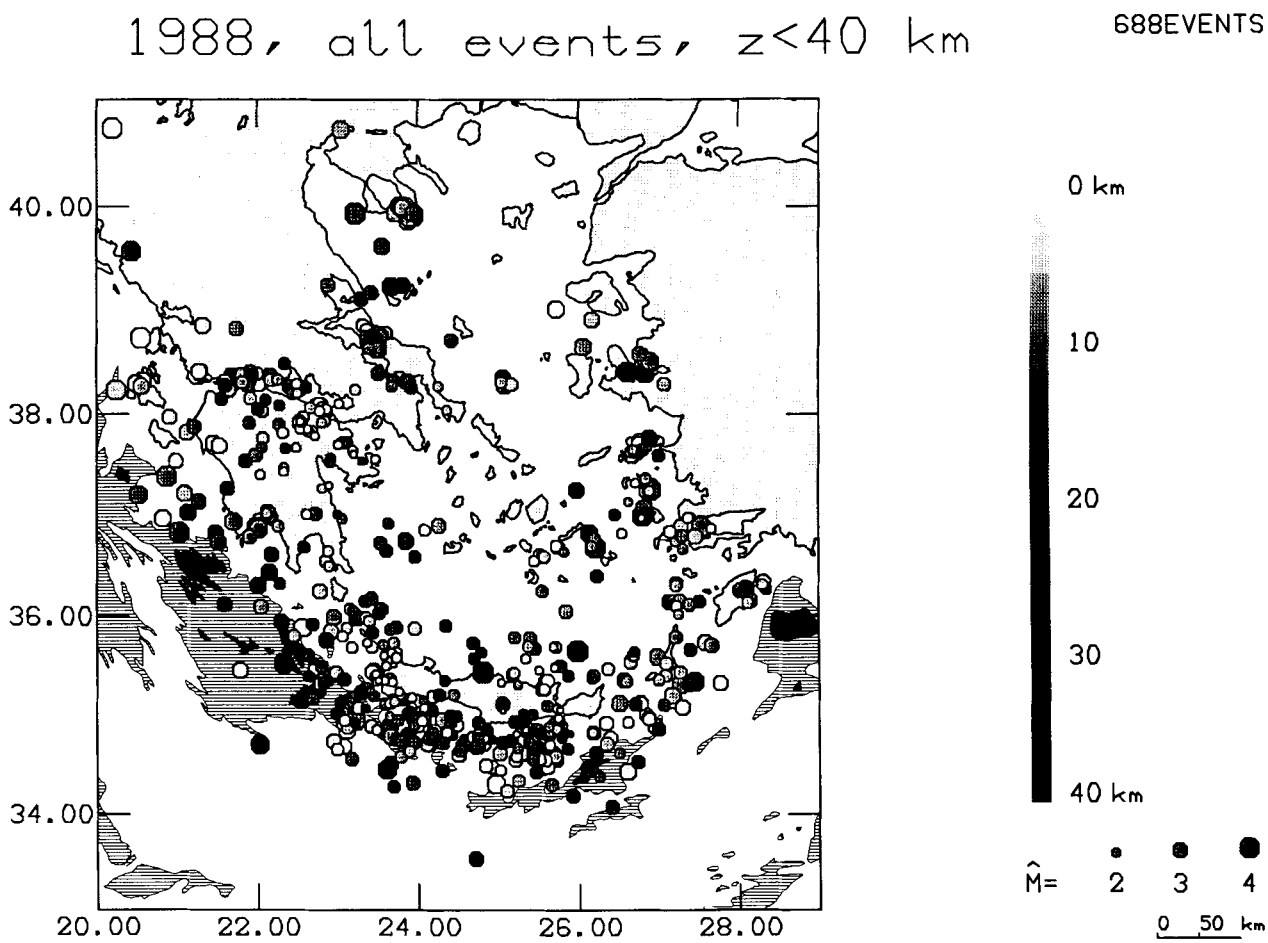

Figure 2. Seismicity map of all 688 events considered to have occurred within the crust.

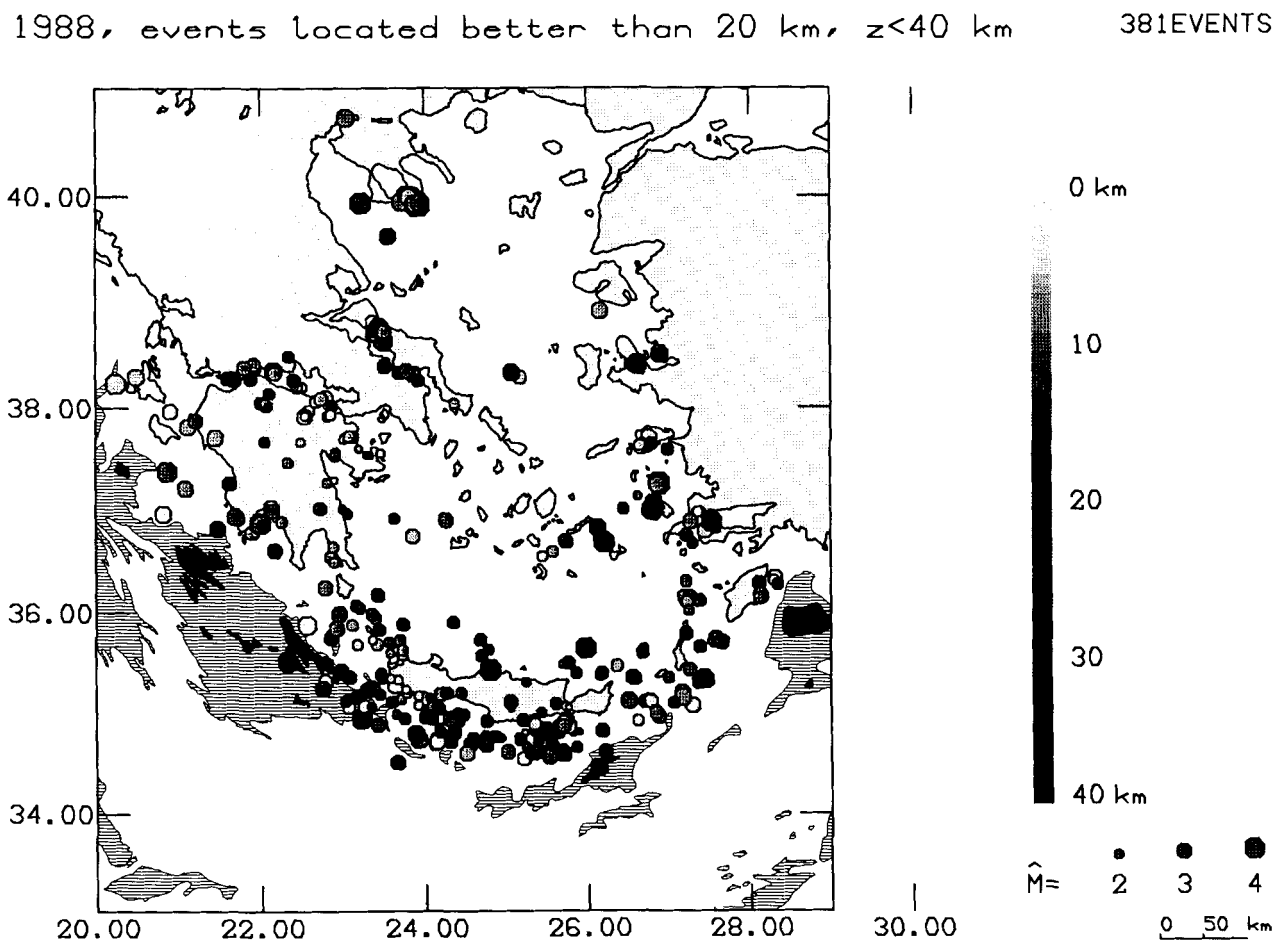

Figure 3. Seismicity map of the 381 selected events (see text) that are located with uncertainties less than 20 km.

4.2 in Chalkidiki, northern Evvia, eastern Peloponnese, northern Crete, and western Turkey. Each was followed by an aftershock sequence of up to several tens of events. A detailed map of the aftershock sequences shows that the scatter in the aftershock epicentres is less than 10 km and confirms that the precision of our locations is indeed within 20 km (Fig. 4). A general map of the 65 focal mechanisms computed (Fig. 5) shows mostly normal faulting. We will now examine separate regions in detail.

Eastern Peloponnese (Figs 6a and b)

The 1988 seismicity map of Peloponnese is neither as precise nor as complete as the one obtained from a more dense network in 1986 surrounding the whole of Peloponnese (Hatzfeld *et al.* 1989). We nevertheless observe seismicity around the Gulf of Corinth and Gulf of Patras, where major earthquakes have occurred several times during this century, with the latest in 1981 (King *et al.* 1985). We were unable to compute many fault plane solutions for earthquakes in this region in 1988, because many of the earthquakes occurred outside of our network.

We also observe some seismicity around Kalamata, where a destructive earthquake of magnitude $Ms = 5.8$ occurred in 1986 (Lyon-Caen *et al.* 1988; Papazachos *et al.* 1988). This seismicity shows that the region is still active, whereas no abnormal pattern was observed during the few weeks preceding the earthquake (Hatzfeld *et al.* 1990). Fig. 6(b) shows two focal mechanisms (events 207 and 223), with extension trending NW–SE consistent with the mechanism of the main shock of 1986 and the mechanisms of small earthquakes in this area in 1986 (Hatzfeld *et al.* 1990).

Seismic activity is also observed in Attiki and in Evvia. One of the strongest earthquakes ($Md = 3.8$) during the experiment was located west of Evvia, close to the Atalanti fault, which strikes NW–SE and broke in 1894 with an earthquake of magnitude $Ms = 7.0$ (Papazachos & Papazachos 1989). Neotectonic studies in this region show normal faulting with extension trending NW–SE on E–W trending faults (Mercier *et al.* 1976). Two fault plane solutions that we computed during this experiment (events 69 and 95) show clear normal faulting, with the T axes trending roughly NW–SE. No teleseismically reliable fault plane solution has been computed in this area, so we can compare our results only with neotectonic observations. In Attiki we recorded

Table 1. Parameters of the focal mechanisms.

1988, all events, z<40 km

N°	Date & Time	Lat	Long	Z	Mag	Plan1		Plan2		P Axis		T Axis	
		°N	°E	km		Az	Pl	Az	Pl	Az	Pl	Az	Pl
30	880711 15:54	35.07	25.73	7.7	1.8	89	30	280	60	6	15	202	74
69	880713 10:39	38.73	23.44	9.0	3.8	28	44	270	64	227	53	333	11
71	880713 11:22	35.06	25.77	13.3	1.6	125	54	308	35	216	9	31	79
95	880714 13:18	38.73	23.41	14.5	3.6	17	49	270	69	226	44	328	12
97	880714 17: 8	37.71	23.03	17.4	2.0	49	70	320	89	273	13	6	13
103	880714 20:40	37.70	23.01	13.2	2.0	160	49	339	40	250	4	70	85
123	880715 12:39	36.69	25.74	15.0	2.8	280	70	30	46	234	46	340	14
127	880715 17:44	37.00	26.80	11.8	2.3	305	60	189	53	160	50	66	3
130	880715 19:25	35.02	25.31	27.5	1.9	230	70	139	89	93	13	186	13
134	880715 22:55	35.69	25.71	8.9	2.4	157	49	4	43	5	76	260	3
180	880719 21:32	36.15	27.51	33.4	2.6	184	70	4	20	93	65	274	24
184	880720 2: 9	35.82	24.97	24.0	2.8	140	49	320	40	50	85	230	4
207	880723 9:19	36.88	22.00	15.5	4.1	57	60	164	63	22	42	290	1
212	880724 6: 2	36.76	23.84	15.8	3.0	130	70	240	46	84	46	190	14
223	880724 22:20	36.87	22.01	16.7	3.6	235	49	44	40	186	83	320	4
231	880725 11:11	34.88	25.75	7.9	3.4	40	49	219	40	310	85	130	4
235	880725 14:45	35.40	26.18	17.5	2.6	0	20	230	76	307	30	159	55
239	880725 20:47	36.75	23.86	6.3	2.9	94	5	270	85	0	40	179	49
256	880726 17:25	36.59	25.56	.5	2.7	99	49	329	52	302	62	35	1
261	880726 21:56	36.11	27.21	13.9	2.6	0	40	209	53	171	73	286	7
262	880726 23:40	36.15	27.20	14.7	2.8	130	40	15	70	325	51	79	17
265	880727 5: 0	35.44	24.81	28.7	4.1	155	68	254	70	115	29	24	0
268	880727 10:55	35.50	25.76	24.4	2.6	192	41	349	50	200	78	90	4
291	880730 6:46	36.16	28.14	19.4	3.1	130	49	300	40	215	4	81	83
306	880731 21:39	36.11	27.38	22.7	2.5	94	54	281	35	187	9	349	79
320	880801 16:45	35.73	23.70	17.3	2.4	230	60	10	37	183	66	303	12
329	880802 11:25	35.50	23.60	12.7	1.9	300	40	120	50	210	5	30	84
342	880803 8: 9	35.73	24.68	18.6	2.5	240	80	145	63	10	10	105	25
357	880804 5:26	35.45	23.45	27.3	3.1	270	49	49	47	247	68	340	1
359	880804 6: 0	36.16	27.26	18.5	2.5	140	30	320	60	49	15	229	75
363	880804 11:43	35.34	23.67	1.3	2.0	80	49	199	59	318	5	55	54
369	880804 18:43	35.23	23.29	29.4	2.9	60	60	245	30	323	74	151	14
378	880805 5:21	35.17	23.18	21.2	2.9	70	40	250	50	159	84	340	5
384	880805 12:53	35.65	25.99	25.4	4.0	179	57	324	38	137	69	254	9
390	880805 22:37	36.10	27.23	12.0	2.4	295	10	115	80	205	35	24	55
394	880806 4:21	35.31	27.38	25.8	2.8	150	80	240	89	105	7	14	7
442	880809 12:34	37.77	26.89	32.3	3.2	344	54	160	35	72	9	266	79
445	880809 13: 9	37.63	26.72	21.5	3.1	10	49	164	42	88	3	342	76
457	880810 1: 6	35.13	23.12	20.2	2.9	40	49	250	44	245	74	144	3

Table 1. (*Continued.*)

1988, all events, z<40 km (continued)

N°	Date & Time	Lat	Long	Z	Mag	Plan1		Plan2		P Axis		T Axis	
		°N	°E	km		Az	Pl	Az	Pl	Az	Pl	Az	Pl
538	880813 22:29	35.59	26.99	13.0	3.3	310	44	120	45	214	0	307	84
542	880814 2:30	35.44	23.42	3.9	2.9	160	20	328	70	231	64	61	25
547	880814 7:27	37.27	26.88	19.5	3.0	99	49	260	41	68	79	180	4
548	880814 7:28	37.25	26.91	16.8	3.7	109	49	290	40	20	85	200	4
555	880814 13:28	35.58	23.73	10.5	2.2	261	30	128	68	202	20	69	61
556	880814 16:13	35.55	23.62	10.6	2.1	270	30	89	60	180	15	0	75
570	880815 5:37	35.35	23.58	8.1	1.9	199	70	20	20	109	65	290	24
579	880815 20: 8	35.12	25.05	20.2	2.8	140	49	280	47	210	1	117	68
597	880816 21:34	39.92	23.94	17.0	4.5	145	35	314	54	198	79	48	9
605	880817 2:10	37.26	26.89	20.8	4.3	70	40	250	50	159	84	340	5
616	880817 12: 8	37.72	23.11	17.5	2.5	295	60	115	30	204	75	24	14
631	880818 9: 1	36.99	26.81	13.9	3.6	88	51	237	42	56	73	164	5
634	880818 10:13	36.99	26.80	15.1	3.3	109	41	265	50	115	76	6	4
637	880818 12: 0	37.73	23.08	11.9	2.4	290	30	109	60	20	75	200	15
638	880818 13:10	34.95	23.22	23.1	3.8	214	51	2	42	184	72	289	4
643	880818 18: 7	35.12	23.59	22.1	2.4	86	48	345	79	42	19	296	37
652	880819 1:52	37.25	26.87	10.0	3.2	260	49	93	40	122	82	356	4
662	880819 17:12	35.98	23.35	19.0	2.5	240	70	60	20	149	65	330	24
684	880820 14:29	35.69	23.42	13.0	2.5	169	40	7	51	325	79	89	5
686	880820 15:32	35.77	25.39	16.0	2.8	160	60	44	53	15	50	281	3
696	880821 3:45	36.82	27.25	18.9	3.1	329	75	150	15	59	29	239	60
715	880821 15:23	37.00	26.79	16.2	3.8	20	49	139	59	355	54	258	5
719	880821 19:51	39.93	23.90	18.2	3.6	132	49	265	50	109	64	18	0
720	880821 21:25	36.98	26.81	15.6	3.2	10	44	179	45	7	84	274	0
728	880822 11: 5	35.83	23.43	27.4	2.5	209	30	0	63	241	68	100	17
761	880824 12:13	36.69	26.21	18.1	4.0	157	49	270	65	131	47	30	9

only a few events. The four focal mechanisms in Argolida are of different types: one reverse fault (event 103) with a *P* axis trending E–W, two normal faults with *T* axes trending N–S, and one strike-slip fault with the same orientations of *P* and *T* axes. There are no mechanisms computed for strong shocks in this area; the closest are from the Gulf of Corinth in 1981 (King *et al.* 1985) and show E–W trending normal faulting and N–S extension. The solutions for the smaller earthquakes in 1988 are therefore consistent with the general strain pattern observed in this area.

We also located a few earthquakes beneath southern Peloponnese and the Cyclades and north of the Argolide basin, which is bounded by ENE–WSW trending normal faults (Angelier *et al.* 1982; Mascle & Martin 1990) One solution (event 212) shows normal faulting with the *T* axis trending N–S; another (event 239) shows either slip on a vertical E–W striking plane, or slip on a horizontal plane.

The Kythira Strait and southwestern Crete (Figs 7a and b)

The Kythira Strait is located between Peloponnese and Crete. It is a bathymetric high separating the Sea of Crete and the Ionian Sea. Kythira and Antikythira are the main islands underlying this topographic feature, but there are also many small islands trending NW–SE. The Kythira Strait belongs geologically to the system of Hellenic nappes but it is characterized by many extensional features. Sea beam surveys (Huchon *et al.* 1982) and seismic reflection surveys (Jongsma *et al.* 1977; Le Quellec *et al.* 1980) show

clearly that the Kythira Strait is a horst structure bounded by normal faults. The trend of the faults (N170°, and therefore oblique relative to the topography) indicates that this region is probably under extension with a slight component of dextral motion in a large-scale *en échelon* system (Lyberis *et al.* 1982). This region has been a seismic gap for strong earthquakes during the last two centuries (Ambraseys 1981; Wyss & Baer 1981; Papazachos & Comninakis 1982).

The level of seismicity recorded during our experiment around the Kythira Strait was relatively high, as it was during the 1986 investigation also. This indicates that the gap is limited to strong earthquakes, but the region continues to deform. The depth of the earthquakes is mostly shallower than 10 km. The epicentres trend approximtely N–S, as do the faults, and are likely to be related to these faults.

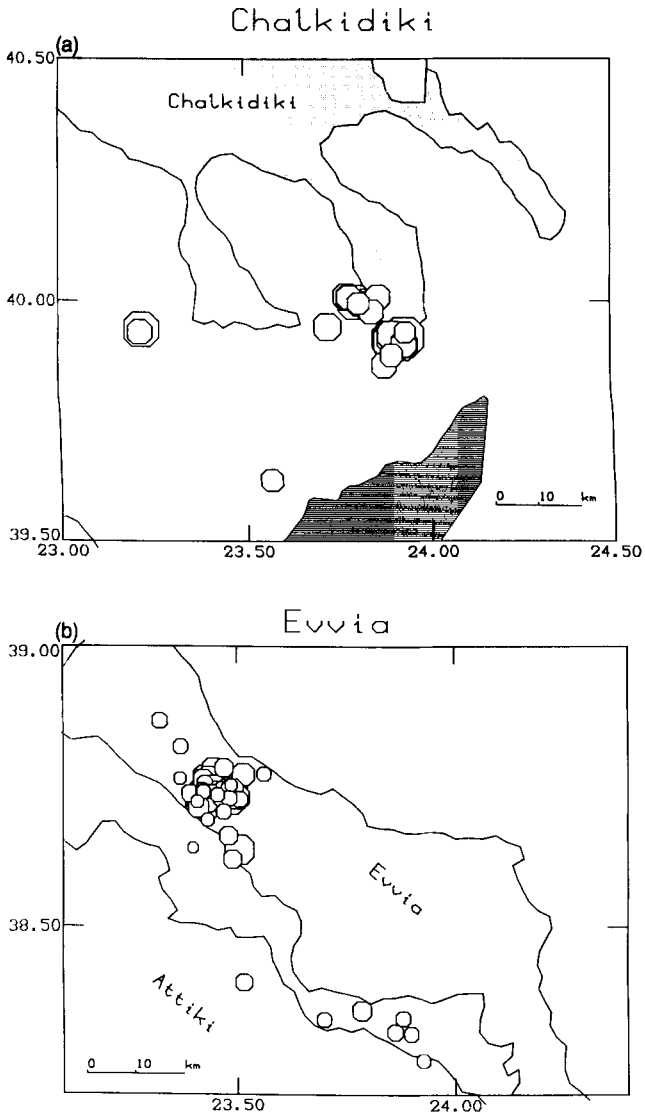

Figure 4. Aftershock sequences of some of the strongest earthquakes recorded during our experiment. The aftershocks show the scatter in location which is likely to be within 10 km. (a) Chalkidiki; (b) Evvia; (c) Leros and Kalymnos.

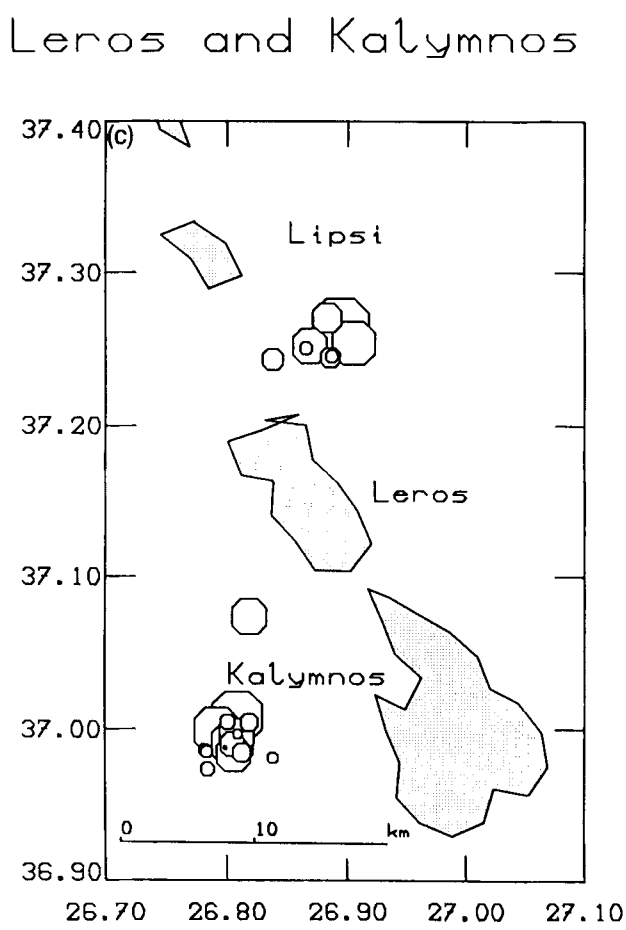

Figure 4. (*Continued.*)

We computed several mechanisms of earthquakes in this region that define two main families of solutions: reverse faulting and normal faulting (Fig. 7b). South-west of Crete, close to the trench, four solutions (events 369, 378, 457 and 638) show normal faulting with *T* axes trending NW–SE, and therefore parallel to the local strike of the trench and perpendicular to the displacement of Aegea relative to Africa. North-west of Crete, around the Kythira Strait, we observe normal faulting again, but with *T* axes trending approximately E–W (events 320, 357, 542, 570, 684 and 728). The E–W normal faulting that is observed west of Crete is consistent with the results obtained by de Chabalier *et al.* (1992), using *S*-wave polarization, during an investigation that followed ours. This type of faulting is also consistent with the focal mechanism of 1965 April 27 (Lyon-Caen *et al.* 1988). Reverse faulting (events 329, 555 and 556) is observed within western Crete, and is well constrained, with *P* axes trending N–S. In this region, we thus observe two types of mechanisms: roughly E–W extension, consistent with tectonic observations on land (Armijo, Lyon-Caen & Papanastassiou 1991, 1992) and NNE–SSW shortening, consistent with the focal mechanisms of larger earthquakes of the Hellenic trench (Taymaz *et al.* 1990).

Crete (Figs 7a and b)

Very little seismic activity was located within Crete (Fig. 7a). A dense network of about 30 stations was installed during the first half of the investigation in eastern Crete, and during the second half in western Crete. These networks were designed to obtain fault plane solutions of shallow earthquakes at both ends of Crete for comparison with neotectonic observations. We did not record many events related to the normal faults clearly visible in eastern Crete (Angelier 1979). Instead, most of the earthquakes occurred south of Crete, between the trench and the coast. South-west of Crete, earthquakes surround the Gavdos Ridge, which is the southernmost continental part of Europe. Further east, earthquakes were located around the Chrisi Ridge (Fig. 7a). The seismicity seems to be restricted to the bathymetric high, rather than to the trench, and no events were located more than 50 km south of the trench. North of Crete, the earthquakes seem again to be restricted to the high topography, and only a few events were located within the deepest part of the Sea of Crete, which consists of small basins (about 50 km wide and 1000 to 2000 m deep) limited by steep scarps (Jongsma *et al.* 1977; Angelier *et al.* 1982; Mascle & Martin 1990).

For eastern Crete, *sensu stricto*, we computed only four mechanisms. Three of them (events 30, 71 and 579) show reverse faulting with P axes trending NNE–SSW. One (event 130) shows strike-slip faulting with a similar orientation of the P axis. North of Crete, most mechanisms (events 134, 184, 268, 384 and 686) show normal faulting with T axis trending E–W. Two solutions show strike-slip faulting, but whereas event 342 is consistent with the T axis trending E–W, this is not the case for event 265, which is located in northern Crete at a depth of 28 km. As for western Crete, we observe mainly E–W extension and NNE–SSW shortening.

The Levantine trenches and the Karpathos Basin (Figs 7a and b)

South-east of Crete are two important bathymetric features; the Pliny trench and the Strabo trench, which are narrow elongated basins trending NE–SW. They are identified as the Levantine branch of the Hellenic arc. Results of seismic reflection profiling (Lêité, Mascle & Anastasakis 1980; Mascle *et al.* 1982; Mascle, Le Cleac'h & Jongsma 1986), sea beam topographic mapping (Huchon *et al.* 1982), and diving

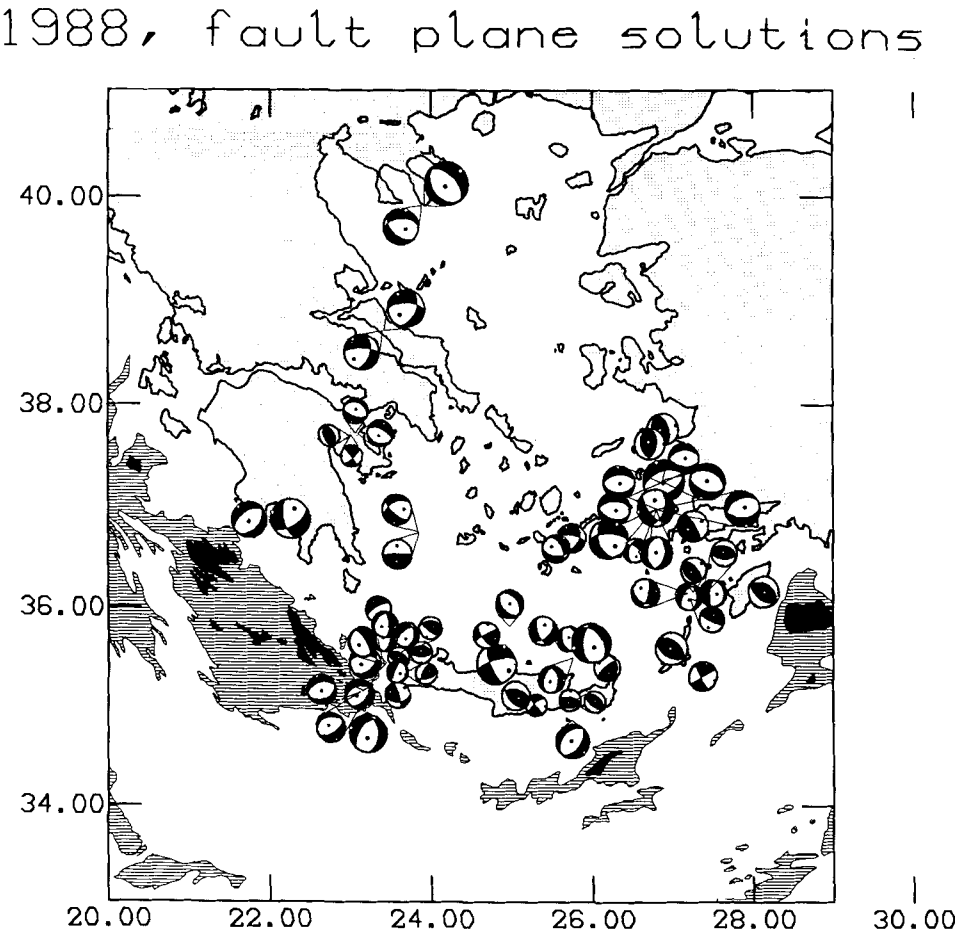

Figure 5. General map of the shallow fault plane solutions. Dark quadrants are compression, light quadrants are extension. The diameter of the balloons is proportional to the magnitude of the earthquakes.

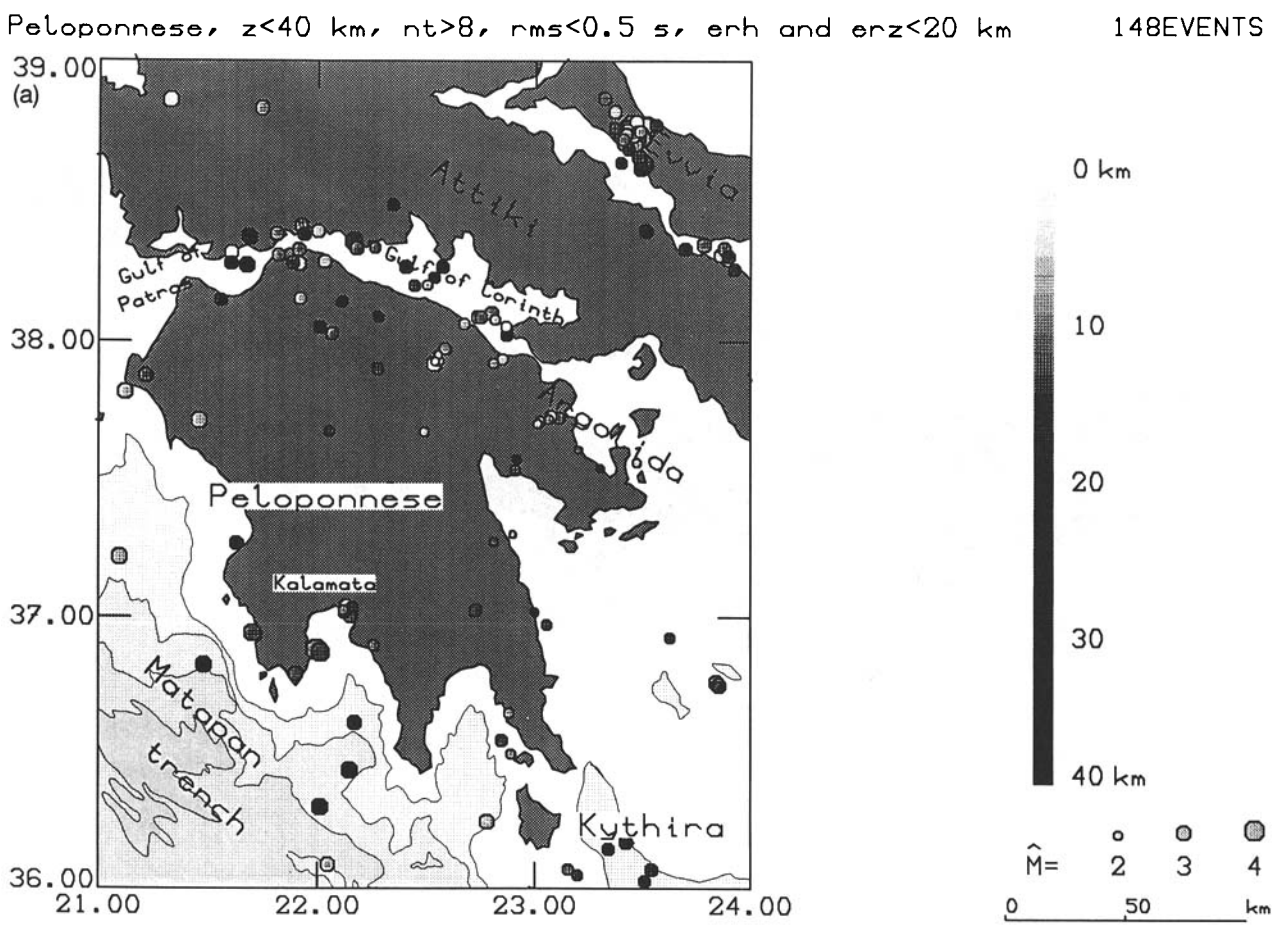

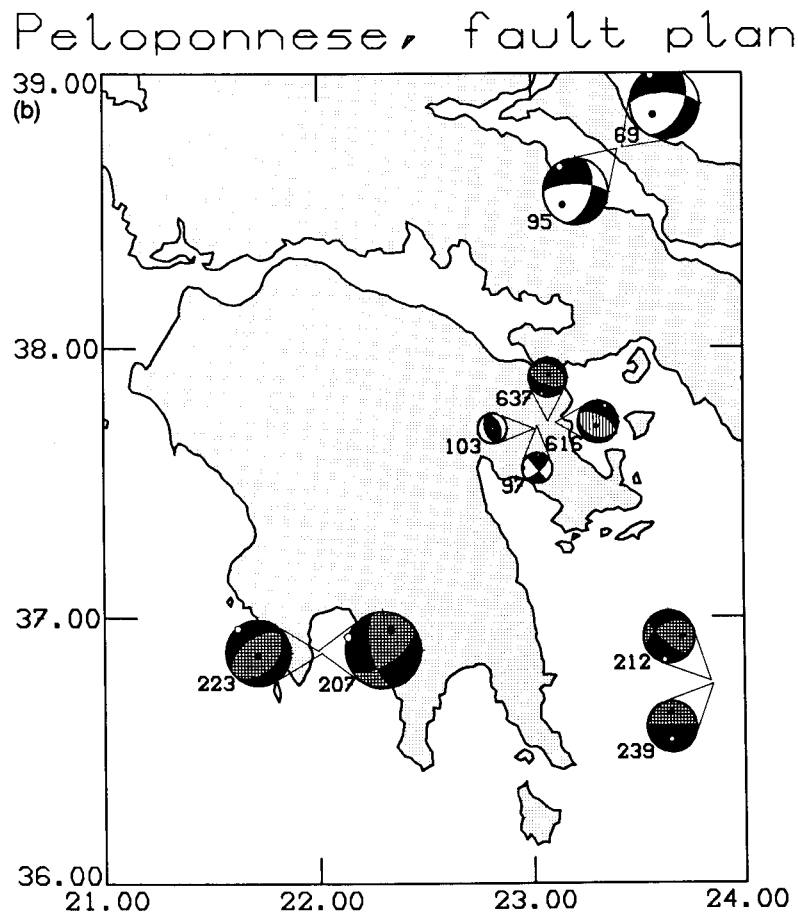

Figure 6. Western Hellenic arc. (a) Reliably located seismicity (uncertainties smaller than 20 km). The bathymetry is shown by 1000, 2000, 3000 and 4000 m contours. (b) Focal mechanisms. Same symbols as for Fig. 5. In the light quadrants, no shade indicates cases for which both planes are constrained within 20°; vertical shading represents only one plane being constrained; a gridded pattern indicates that only *P* and *T* axes are constrained.

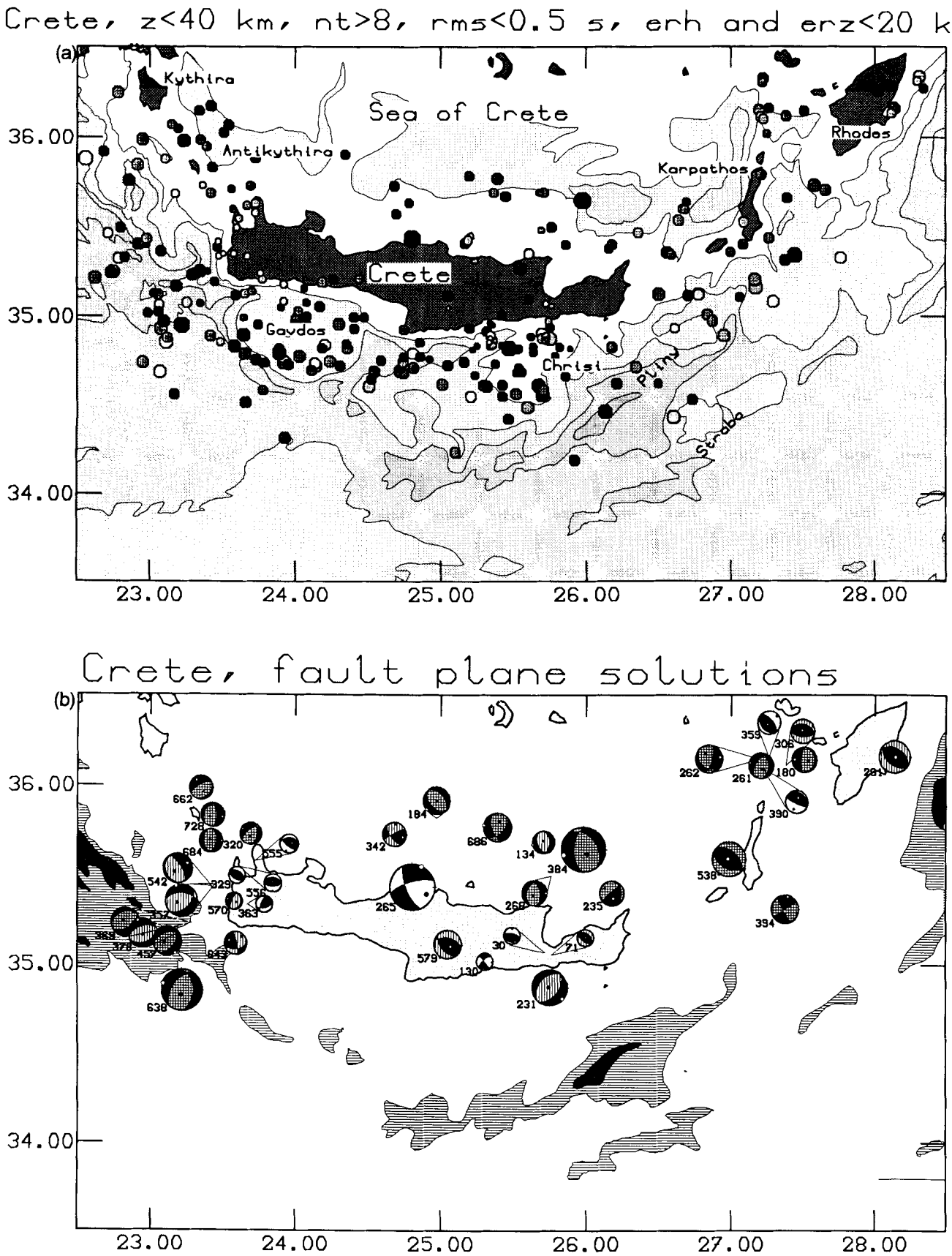

Figure 7. Crete and region. (a) Seismicity map. Note that reliably located seismicity is located north of the Hellenic trench. Very little activity was located within Crete. (b) Focal mechanisms. Same symbols as for Fig. 5. N–S to NW–SE extension is observed in western Crete, but E–W extension in northern–eastern Crete as in the Dodecanese islands. From place to place we also observe NE–SW compression.

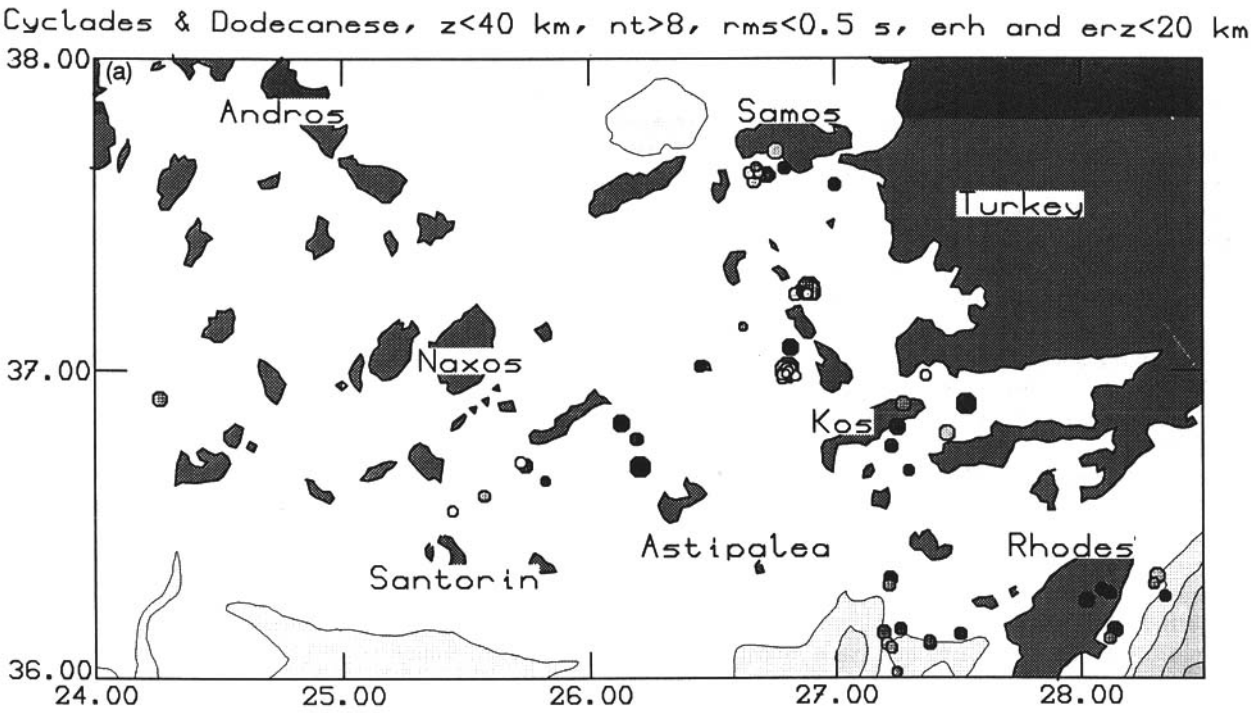

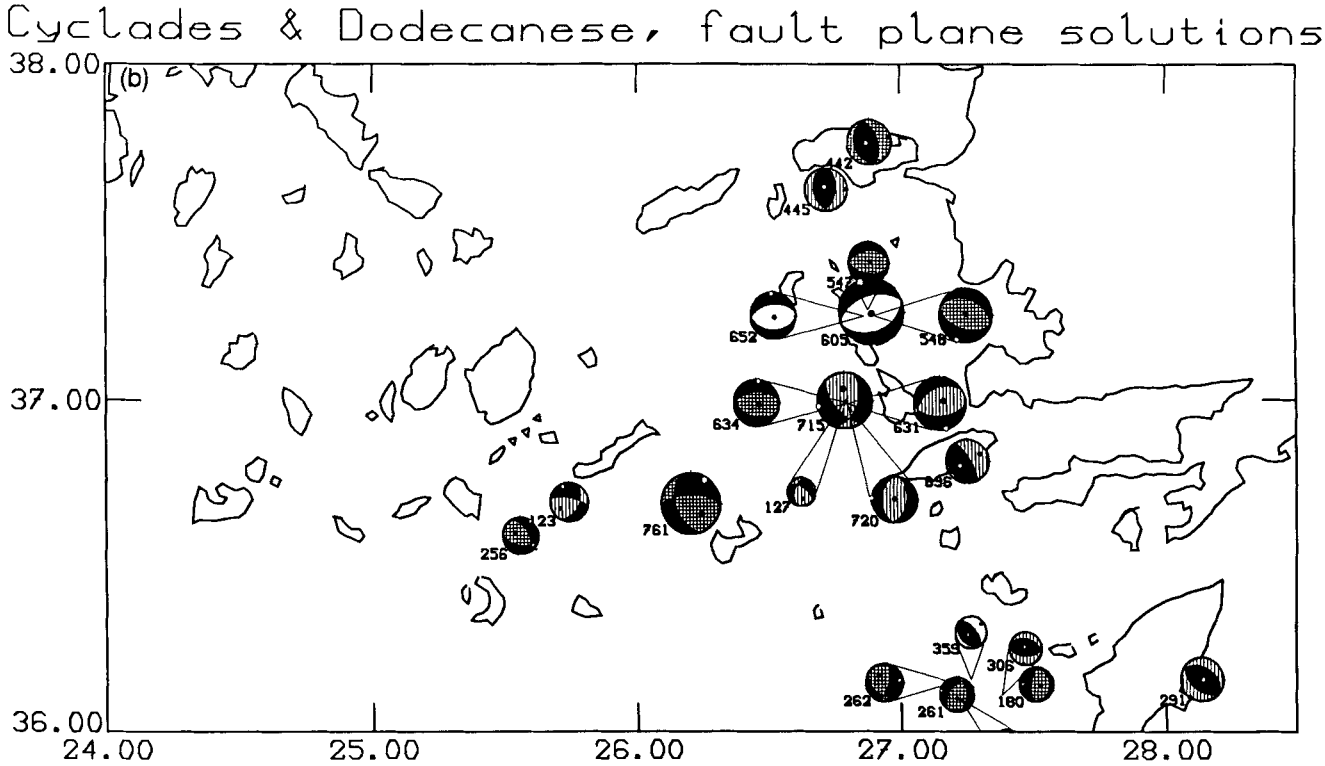

Figure 8. Cyclades and Dodecanese Islands. (a) Seismicity: only very little seismic activity was located between Naxos and Astipalae; most of the earthquakes were located around the Dodecanese Islands. (b) Focal mechanisms. Same symbols as for Fig. 5. North of the Dodecanese islands we observe both E–W compression and N–S extension, but in the southern Dodecanese Islands we observe the reverse, NNE–SSW compression and E–W extension.

observations (Le Pichon *et al.* 1981) suggest that the morphology of the Levantine branch is different from the Ionian branch. The Ionian branch located to the west of Crete is thought to undergo only compression, whereas the Levantine branch is thought to undergo both left-lateral strike-slip and reverse motion.

Most of the earthquakes that we recorded were located north of the Pliny trench. Results from an experiment conducted with five ocean bottom seismographs (Kovachev, Kuzin & Soloviev 1992), located in the same area also show only little activity located between the two trenches and restricted to the eastern part. It is, therefore, likely that the active boundary is related to the Pliny trench and not to the Strabo trench.

Only one fault plane solution (event 394), showing dextral strike-slip solution, if we choose the NE–SW trending plane, can be linked with the Pliny trench. This motion is the reverse of what is expected from the displacement between the Hellenic arc and the Africa plate (McKenzie 1972, 1978; Le Pichon & Angelier 1979), but it is consistent with the only available focal mechanism of a moderate earthquake clearly related to the Strabo trench on 1985 September 27 (Taymaz *et al.* 1990; Liakopoulou *et al.* 1992). Among other solutions computed for earthquakes located farther north, Within the Karpathos basin, most (events 291, 306, 359, 390 and 538) show reverse faulting with *P* axes trending NE–SW, but a few (events 180 and 262) show normal faulting with extension in the perpendicular direction.

The Cyclades and Dodecanese Islands (Figs 8a and b)

Less is known about this part of the Cretean Sea than about the central area. The morphology of the sea bottom suggests tectonics similar to those in western Turkey (Mascle & Martin 1990), and normal faulting with N–S extension is present. The few events (less than 10) that we recorded within the Sea of Crete were located between Naxos and Astipalea. More activity was recorded farther east around the Dodecanese Islands, especially between the islands of Samos and Kos. In the Cyclades, the two computed mechanisms (events 123 and 256) show normal faulting with roughly N–S trending *T* axes. Around Samos, two mechanisms (events 442 and 445) show reverse faulting with *P* axes trending E–W. Farther south we observe normal faulting either with N–S extension (events 547, 548, 605, 631, 634 and 652), or with E–W extension (events 127, 715 and 720). The few focal mechanisms of larger earthquakes in this area (McKenzie 1972, 1978) show mainly NW–SE to N–S extension, as for earthquakes in western Turkey.

DISCUSSION

In regions of moderate seismicity, as in the Mediterranean, the number of earthquakes of large magnitude, for which teleseismic locations and fault plane solutions are reliable, is small. If the geodynamics are complex, these mechanisms are often insufficient to answer some basic questions. The installation of a dense temporary network allows the recording of a greater number of earthquakes, usually with more precisely determined epicentres and depths, than those based on teleseismic recordings. Moreover, for earthquakes with upgoing ray paths, the focal sphere is more completely sampled, and fault plane solutions can be better constrained than for those with teleseismic data. However, because such networks are difficult to maintain and because it is not possible to record for long periods of time, only earthquakes of small magnitude are usually located, and the image of the brittle part of the deformation might not be representative of the long-term deformation. The dimensions of the rupture for an earthquake of magnitude 6 is of the order of 10 km, but that for an earthquake of magnitude 3 is only a few hundred metres. Small earthquakes, therefore, do not rupture the whole brittle part of the crust, and the relationship between the focal mechanisms of microearthquakes and deformation is not as obvious as it is for larger earthquakes because the existence of pre-existing faults probably influences the focal mechanisms greatly. We assume that the heterogeneities due to the previous tectonics are randomly distributed and that smoothing the observations over an area that is comparable in dimensions to one big fault allows us to infer a 'mean' strain pattern. In other words, at this scale, the brittle crust (even composed of heterogeneous material) responds homogeneously to the deformation of the lithosphere, which is related to the large-scale geodynamics of the region. It is therefore crucial to check whether the information provided by small earthquakes is consistent with that provided by strong earthquakes.

In our case the seismicity that we observed during the seven weeks of study is spread over most of the Hellenic arc and does not define a small number of active faults separating aseismic blocks (Figs 2 and 3), and within the area, only the Sea of Crete is aseismic. These observations are consistent with seismicity maps computed from teleseismically located strong earthquakes (Papazachos & Comninakis 1971; Makropoulos & Burton 1984). This is a feature that we commonly observe in the Mediterranean region, and that we also observed in Peloponnese (Hatzfeld *et al.* 1990). Two different seismicity patterns characterize the Mediterranean region: (1) clusters of earthquakes from place to place (e.g. the El Asnam spot in Algeria), or (2) wide zones of distributed seismic activity (as in southern Spain or Italy). In the second pattern the small, but diffuse, deformation could explain this pattern of seismicity, and the diffuse distribution of brittle deformation could be controlled by weakness inherited from previous seismic events. In the case of the Aegean, however, a slow rate of deformation cannot explain the diffuse seismicity, because the deformation is not slow. Recent faulting is widespread, and some faults can be related to strong earthquakes (e.g. Mercier *et al.* 1976; Angelier *et al.* 1982; Armijo *et al.* 1991).

We did not locate earthquakes at distances greater than 50 km south of the Hellenic Trench (Fig. 7a). This is not just because our network was located over the islands of the Aegean Sea, and therefore not favourably situated to locate such earthquakes. We did locate earthquakes near the Matapan trench, west of Peloponnese, at a distance from the network greater than the southern Hellenic trench (Fig. 2). Thus, it is likely that earthquakes south of the trench are

rare, and most of them may be mislocated (Papadopoulos, Wyss & Schmerge 1988). It has been suggested that high topography of the Mediterranean ridge is an accretionary prism in front of the crustal backstop of the Hellenic arc (Le Pichon *et al.* 1982; Truffert *et al.* 1993). In this part of the Hellenic trench located south of Crete, the seismicity does not support the suggestion that the active boundary is located farther than 50 km seaward. It is difficult to test this model with seismicity, because the aseismicity to the far south of the trench does not prove that there is no deformation there: the lower strength of the prism of sediments could prevent seismic slip. The only conclusion that we can draw is that seismicity located within the African plate is low. There have been a few isolated shocks around the Mediterranean ridge and one earthquake (1982 August 17), modelled using body waves by Taymaz *et al.* (1990), exhibits an uncommon focal mechanism and an uncommon depth of 39 km. Such events are evidently not numerous and could be related to stress release within the subducting plate and not at the interface.

The Sea of Crete is not seismically active either (Fig. 7a). This is consistent with the teleseismically located seismicity for the last 20 years, but it is surprising given the internal deformation that this region has experienced since the Pliocene (Mercier *et al.* 1989; Angelier *et al.* 1982) Bouguer gravity anomalies (Makris & Stobbe 1984), bathymetry (Morelli, Pisani & Gantar 1975), and seismic reflection profiles (Huchon *et al.* 1982; Mascle & Martin 1990) suggest that the crust in this region has been stretched and thinned by a factor of up to 2 (Angelier *et al.* 1982). It is not obvious to relate the lack of seismicity in the Cretean Sea to the collision of the Hellenic arc with the continental shelf of Africa (Lyon-Caen *et al.* 1988), to the migration and cooling of the region of high strain (Sonder & England 1989), or to the uprising of the geotherm due to the thinning of the crust which favours ductile rather than brittle deformation.

Our focal mechanisms agree with those of strong earthquakes in many areas: normal faulting and N–S extension around Corinth, like that of the 1981 sequence (Jackson *et al.* 1982; King *et al.* 1985); NW–SE extension around Kalamata and in the Kythira Strait, like that of the Kalamata earthquake and the 1965 earthquake in NW Crete (Lyon-Caen *et al.* 1988; Papazachos *et al.* 1988); dextral strike-slip motion near the Pliny trench, which though puzzling is similar to the only mechanism teleseismically computed in this area (Taymaz *et al.* 1990; Liakopoulou *et al.* 1992); and N–S extension north of the Dodecanese Islands as in the results of McKenzie (1972, 1978). As a consequence we think that our results are credible in the places where we do not have information from strong earthquakes, at least when we smooth and consider the average strain over an area whose dimensions are similar to those of large earthquakes. The total picture of small magnitude earthquake mechanisms that we get in the Aegean is no more scattered than the picture that we get from larger earthquakes.

The results showing extension along the Hellenic arc are not inconsistent with the reverse faulting generally reported in this area. Our observations apply to the arc itself, where our stations were located, whereas the reverse faulting reported by others (McKenzie 1972, 1978; Taymaz *et al.* 1991) is observed more seaward along the trench, where the major earthquakes are located. One way to smooth our observations is to determine the mean orientations of the principal axes of deformation (*P* and *T* axes), at least for those that plunge at gentle angles. In the following we assume that the orientations of the *P* and *T* axes reflect orientations of compressional and extensional strain.

Figures 9(a) and (b) show respectively the horizontal projections of the shallowly plunging *P* and *T* axes (plunge $<45°$). On the same map we show the observations found in the literature for strong earthquakes (e.g. McKenzie 1972, 1978; Anderson & Jackson 1987; Lyon-Caen *et al.* 1988; Taymaz *et al.* 1990, 1991). Subhorizontal *P* axes are located mostly along the Hellenic trench, and most of them trend roughly perpendicular to the trench. The pattern of reverse faulting, located across the boundary between the two plates, is consistent with the underthrusting of the African plate beneath the Aegean. Along the trench, the trend of the *P* axes varies from ENE–WSW in the north-western part to NNE–SSW in the southern part. This variation is consistent both with a clockwise rotation of 30° of the Hellenic arc relative to the African plate about a nearby pole at 40°N and 18°E (Le Pichon & Angelier 1979; Kissel & Laj 1988), or with internal extensional deformation of the arc.

The *T* axes show more variety, for both the small and large earthquakes. They trend N–S in the northern Aegean Sea, around Evvia and the Gulf of Corinth, in the Cyclades and in the Dodecanese Islands. The trend of the *T* axes is therefore constant, in the northern Aegean Sea, and roughly parallel to the relative motion between Aegea and Africa (e.g. Jackson & McKenzie 1988). The *T* axes of earthquakes along the Hellenic arc, however, trend parallel to the trench: south of Peloponnese and in western Crete the *T* axes trend NW–SE, but in eastern Crete and in the Dodecanese Islands the *T* axes trend roughly E–W.

The smaller earthquakes are located on the internal part of the Hellenic trench and complement the deformation observed in the northern Aegean Sea and the Hellenic trench. They extend the results observed for the western part of the Hellenic arc during 1986 (Hatzfeld *et al.* 1990). They are consistent with most of the neotectonic observations (Mercier 1981; Angelier *et al.* 1982). This strain pattern, deduced from small magnitude earthquakes, is neither uniform nor isotropic and confirms that the Aegean is experiencing an important amount of internal deformation. The radial extension in northern Aegea and the longitudinal extension along the boundary between the two plates suggest a process similar to the mechanisms of gravity nappes (Merle 1989). The radial extension is related to the southward flow of the Aegean lithosphere and the tangential extension is due to volume conservation as the lithosphere spreads outward.

Taymaz *et al.* (1991) proposed a model of broken slats to explain the deformation observed in the northern and central Aegean Sea. This model is based on mechanisms of earthquakes for the northern Aegean Sea. The westward motion of Turkey relative to Europe plays a major role in initiating the deformation which is not self-sustaining because of the subduction of the African plate beneath the Aegean. The cause of this gravity spreading nappe could be

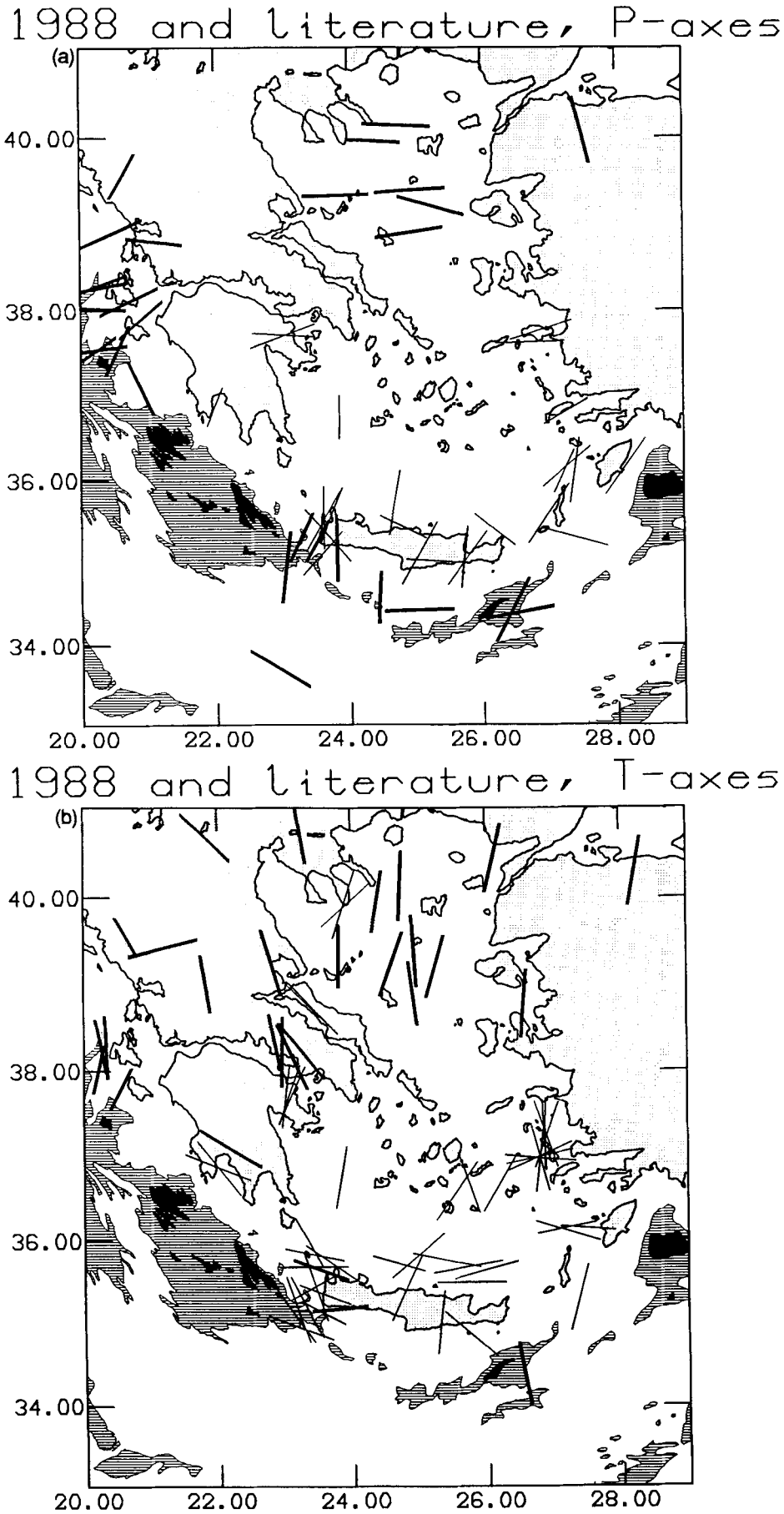

Figure 9. Map of principal axes of the deformation deduced from the focal mechanisms. Thin lines are for data from this study, and thick lines are for mechanisms taken from the literature (see text). We represent the horizontal projection of the axes which plunge less than 45°. (a) *P* axes trend mostly NE–SW for the western Hellenic arc but NNE–SSW for the southern Hellenic arc. (b) *T* axes trend N–S for the north Aegean Sea, the Cyclades and the north Dodecanese Islands. They trend parallel to the Hellenic arc for the mechanisms located on the periphery.

seen in the difference of the topography between the Aegean Sea and the Mediterranean Sea (Berkhemer 1977), but also in the sinking of the slab within the asthenosphere (Le Pichon & Angelier 1979), which maintains the extension within the overriding plate (Sonder & England 1989). The model of Taymaz *et al.* (1991) is also consistent with rotation in an opposite sense of both sides of the Hellenic arc (Kissel & Laj 1988).

Our results for the South Aegean Sea, of dimensions comparable to those of the North Aegean Sea, show that the deformation is different in the southern part from that in the north. Summing the moment tensors for the earthquakes of the last 70 years, Jackson & McKenzie (1988) found that the total average annual seismic moment rate is about 249×10^{24} dyn. cm yr^{-1} for the North Aegean and western Turkey, but is only 85×10^{24} dyn. cm yr^{-1} for the Hellenic trench. These values correspond to a velocity of 34–113 mm yr^{-1} between the Hellenic arc and Eurasia across the northern Aegean but only 3–13 mm yr^{-1} of convergence between the Hellenic trench and Africa, which compared to the predicted values of 70 mm yr^{-1} and 100 mm yr^{-1} respectively, shows an important difference in the style of deformation.

Using the azimuth of the slip vector along the Hellenic arc, Le Pichon & Angelier (1979) proposed a kinematic model of rotation of the 'Aegea Consuming Boundary', consistent with extension within Aegea. Based largely on mechanisms computed by Ritsema (1974), they reported azimuths of slip vectors of 58° to 48° for the Ionian Islands and of 22° to 17° for the eastern part of the arc. Martin (1988) restricting the mechanisms of Ritsema to the first two best classes, and using the moment tensor solutions of McKenzie (1978) and Dzeiwonski *et al.* (1981–1988), found a slightly different pattern: 40° for the Ionian Islands and 10° for eastern Crete. Using body wave modelling, Taymaz *et al.* (1990) found a mean azimuthal trend of 25° for the earthquakes located around Crete. It seems likely, therefore, that the mean azimuth of the slip vectors is about 40° to 50° for earthquakes located around the Ionian islands, and around 25° for the earthquakes located around Crete. Le Pichon & Angelier (1979) considered that this variation in azimuth is due to the proximity of the pole of rotation to the boundary between Aegea and Africa. But as pointed out by Le Pichon & Angelier (1979), the discrepancies between the measured and predicted values are westward in the west and eastward in the east. This suggests that the 'Aegean Consuming Boundary' does not behave as a rigid boundary but is deforming. Furthermore, palaeomagnetic observations suggest that Crete moved southward without rotation when Peloponnese was rotated 25° ± 12° clockwise (Kissel & Laj 1988), and that the Ionian zone of Albania rotated also (Speranza *et al.* 1992).

We propose an alternative interpretation: assuming that the subduction of the African plate is essentially rigid, the difference in azimuth of slip vectors of about (50° ± 20°) − (25° ± 12°) = −7°, +57° for earthquakes located along the Hellenic trench implies relative motion between Peloponnese and Crete. In a first approximation we consider that the rate of displacement between both Crete and Peloponnese relative to Africa is about 70 ± 30 mm yr^{-1} (Jackson & McKenzie 1988); this gives us a relative divergence between Peloponnese and Crete of about 41 ± 40 mm yr^{-1}, if we take

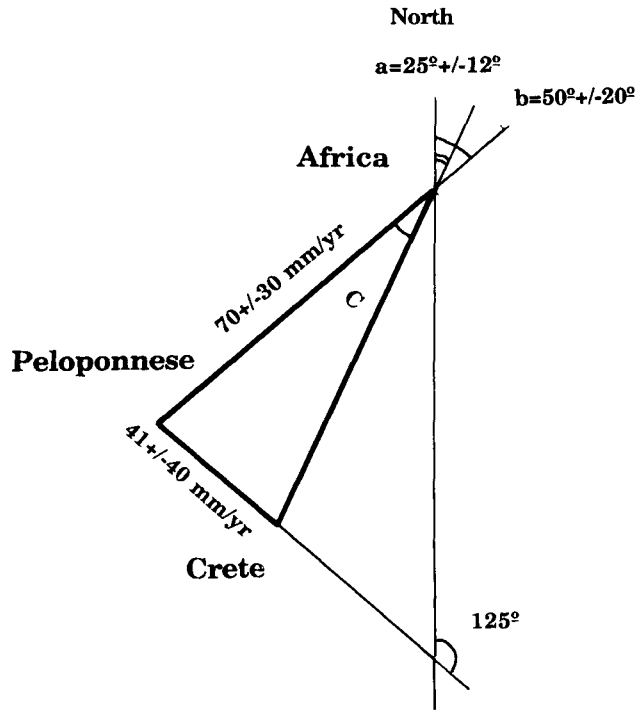

Figure 10. Diagram showing the geometry of relative displacement between Peloponnese, Crete and Africa. The azimuth of *a* is from Taymaz *et al.* (1990), the angle *C* is the difference between the azimuth of the slip vectors for Peloponnese and Crete. The motion between both Crete and Peloponnese relative to Africa is ~70 ± 30 mm yr^{-1}. The relative motion inferred by the geometry is 41 ± 40 mm yr^{-1} and is parallel to the Hellenic trench, suggesting an important amount of internal deformation within the Aegean, consistent with the focal mechanisms of earthquakes in this area.

the extreme values for difference in azimuth (Fig. 10), which is manifested by internal deformation within the Aegean. This deformation could be localized, for instance around the Kythira Strait, as proposed by Lyon-Caen *et al.* (1988). Our results (Hatzfeld *et al.* 1990; this paper), however, suggest that the extension is distributed along the Hellenic arc, because we observe normal faulting all along the arc. An azimuth of 25° for the relative motion between Crete and Africa constrains the orientation of the internal extension within the Aegean to be about 125°. This azimuth is also approximately parallel to the trend of the Hellenic trench, west of Peloponnese, and it is consistent, therefore, with longitudinal extension along the arc (Fig. 10).

CONCLUSION

With a dense network of portable stations installed over the South Aegean, we recorded and located a large number (~800) of earthquakes of small magnitude. Most of our observations concern the internal part of the Hellenic arc, located between the North Aegean Sea and the Hellenic trench. In this region strong earthquakes have been few, and therefore do not define a homogeneous image of the deformation in that area.

Our observations show that the seismicity is located

mainly along the Hellenic arc. The boundary between the subducting African plate and the overriding arc cannot be located farther than 50 km south of the Hellenic trench. Behind the arc we observe seismicity and therefore brittle deformation. This deformation is distributed and not localized on a few important faults, suggesting that some internal brittle deformation (which could represent only 10 per cent of the total deformation) can be accommodated by widespread but small deformation on numerous pre-existing faults. The Sea of Crete which has stretched by a factor of 2 is not actively seismic.

The focal mechanisms that we computed complement those computed for big earthquakes. We observe reverse faulting along the trench in a direction consistent with the relative motion between Aegea and Africa. The difference in the azimuth of the slip vectors of about 25°, for earthquakes located along the trench, between Peloponnese and Crete suggest that internal deformation takes place within the Aegean. The rate of extension is, therefore, about half that between Aegea and Africa and the trend is roughly parallel to the trench. The non-uniform extension that we observe behind the arc is also consistent with the tectonic observations on land, including the palaeomagnetic results, and we suggest that the mechanism of internal deformation observed in the Aegean is similar to a gravity nappe.

ACKNOWLEDGMENTS

We would like to thank all the observers who helped us in maintaining the seismological stations: S. Agelis, V. Alevra, M. Amalvict, M. Bour, M. Chalkiadakis, G. Chatzigianis, P. Chavez-Garcia, I. Cifuentes, M. Cointre, A. Daskalaki, A. Deschamps, G. Drakatos, K. Exarchos, M. Frogneux, P.Guérin, R. Guiguet, G. Karakaisis, K. Karavasilis, I. Kassaras, D. Kementzetzidou, P. Konstantinidou, K. Kortesis, V. Kouskouna, G. Lambaré, J. L. Lecardinal, J. Louis, H. Lyon-Caen, Ch. Martin, G. Michaletos, K. Mouratidis, D. Panagiotopoulos, M. Papachristofis, N. Papadimitriou, I. Papamichos, J. Papasotirioy, K. Paraskevopoulos, L. Polymenakos, S. Roecker, J. C. Ruegg, M. Scordilis, G. Selvaggi, I. Sofoulis, C. Thomas, A. Tsagarakis, M. Tsikalakis, D. Tsintzos, N. Voulgaris, T. Vourakis, N. Vourlakos, G. Zachos. This experiment would not have been possible without the encouragements of J. Drakopoulos and B. Papazachos. S. Perrier helped in processing the data, J. Blanchet and INSU in the bureaucracy. P. Molnar kindly reviewed several versions of the manuscript, and we benefited from the helpful reviews of J. Jackson and S. Roecker. This work has been supported by EEC, Stimulation Contract No. 353.

REFERENCES

Ambraseys, N. N., 1981. On the long term seismicity of the Hellenic arc, *Boll. Geof. Teor. Appl.*, **XXIII,** 355–359.

Anderson, H. J. & Jackson, J. A., 1987. Active tectonics of the Adriatic region, *Geophys. J. R. atr. Soc.*, **91,** 937–983.

Angelier, J., 1979. Néotectonique de l'arc égéen, *Soc. Géol. du Nord,* **3.**

Angelier, J., Lyberis, N., Le Pichon, X., Barrier, E. & Huchon, P., 1982. The neotectonic development of the Hellenic Arc and the Sea of Crete: a synthesis, *Tectonophysics,* **86,** 159–196.

Argus, D. F., Gordon, R. G., DeMets, Ch. & Stein, S., 1989. Closure of the Africa–Eurasia–North America plate motion circuit and tectonics of the Gloria Fault, *J. geophys. Res.*, **94,** 5585–5602.

Armijo, R., Lyon-Caen, H. & Papanastassiou, D., 1991. A possible normal-fault rupture for the 464 BC Sparta earthquake, *Nature,* **351,** 137–139.

Armijo, R., Lyon-Caen, H. & Papanastassiou, D., 1992 East–west extension and holocene normal-faults scarps in the Hellenic arc, *Geology,* **20,** 491–494.

Berkhemer, H., 1977. Some aspects of the evolution of marginal seas deduced from observations in the Aegean region, in *Int. Symp. on the Structural History of the Mediterranean Basins,* pp. 303–314, eds Biju-Duval, B. & Montadert, L., Split, Technip, Paris.

Besnard, M., 1991. Sismotectonique de l'arc égéen, résultats d'une campagne de microsismicité, *Thèse,* l'Université J. Fourier, Grenoble.

Billiris, H. *et al.,* 1991. Geodetic determination of the strain of Greece in the interval 1900 to 1988, *Nature,* **350,** 124–129.

Chatelain, J. L., Roecker, S. W., Hatzfeld, D. & Molnar, P., 1980. Microearthquakes and fault plane solutions in the Hindu Kush region and their tectonic implications, *J. geophys. Res.*, **85,** 1365–1387.

De Chabalier, J. B., Lyon-Caen, H., Zollo, A., Deschamps, A., Bernard, P. & Hatzfeld, D., 1992. A detailed analysis of Microearthquakes in western Crete from digital 3-component seismograms, *Geophys. J. Int.*, **110,** 347–360.

Dziewonski, A., Ekström, G., Franzen, J. E. & Woodhouse, J. H., 1988. Centroïd moment tensor solutions, *Phys. Earth planet. Inter.*, **50,** 155–182.

Ekström, G. & England, Ph., 1989. Seismic strain rates in regions of distributed continental deformation, *J. geophys. Res.*, **94,** 10 231–10 257.

Grange, F., Hatzfeld, D., Cunningham, P., Molnar, P. Roecker, S. W., Suarez, G., Rodriguez, A. & Ocola, L., 1984. Tectonic implications of the microearthquake seismicity and fault plane solutions in Southern Peru, *J. geophys. Res.*, **89,** 6139–6152.

Hatzfeld, D. & Martin, Ch., 1992. The Aegean intermediate seismicity defined by ISC data, *Earth planet. Sci. Lett.*, **113,** 267–275.

Hatzfeld, D., Pedotti, G., Hatzidimitriou, P., Panagiotopoulos, D., Scordilis, M., Drakopoulos, I., Makropoulos, K., Delibasis, N., Latousakis, I., Baskoutas, J. & Frogneux, M., 1989. The Hellenic subduction beneath the Peloponnesus: first results of a microearthquake study, *Earth planet. Sci. Lett.*, **93,** 283–291.

Hatzfeld, D. Pedotti, G., Hatzidimitriou, P. & Makropoulos, K., 1990. The strain pattern in the western Hellenic arc deduced from a microearthquake survey, *Geophys. J. Int.*, **101,** 181–202.

Hatzfeld, D., Besnard, M., Makropoulos, K., Hatzidimitriou, P., Panagiotopoulos, D., Karakaisis, G., Deschamps, A. & Lyon-Caen, H., 1993. Subcrustal microearthquake seismicity and fault plane solutions beneath the Hellenic arc, *J. geophys. Res.*, **98,** 9861–9870.

Huchon, Ph., Lybéris, N. Angelier, J., LePichon, X. & Renard, V., 1982. Tectonics of the Hellenic trench: a synthesis of Sea-Beam and submersible observations, *Tectonophysics,* **86,** 69–112.

Jackson, J. A. & McKenzie, D., 1988. The relationship between plate motions and seismic moment tensors, and the rates of active deformation in the Mediterranean and the Middle East, *Geophys. J.*, **93,** 45–73.

Jackson, J. A., Gagnepain, J., Houseman, G., King, G. C. P., Papadimitriou, P., Soufleris, C. & Virieux, J., 1982. Seismicity, normal faulting, and the geomorphological development of the

Gulf of Corinth (Greece): the Corinth earthquakes of February & March 1981, *Earth planet Sci. Lett.*, **57,** 377–397.

Jongsma, D., Wissmann, K., Hinz, K. & Gardé, S., 1977. Seismic studies in the Cretean Sea. 2. The southern Aegean Sea: An extensional marginal basin without sea-floor spreading? in *'Meteor' Forschungsergebnisse*, Gebrüder Borntraeger eds, **27,** 31–43.

King, G. C. P., Ouyang, Z. K., Papadimitriou, P., Deschamps, A., Gagnepain, J., Houseman, G., Jackson, J. A., Soufleris, C. & Virieux, J., 1985. The evolution of the Gulf of Corinth (Greece): an aftershock study of the 1981 earthquakes, *Geophys. J. R. astr. Soc.*, **80,** 677–693.

Kiratzi, A. A. & Langston, Ch. A., 1989. Estimation of earthquake source parameters of the May 4, 1972 event of the Hellenic arc by the inversion of waveform data, *Phys. Earth planet. Inter.*, **57,** 225–232.

Kiratzi, A. A. & Langston, Ch. A., 1991. Moment tensor inversion of the 1983 January 17 Kefallinia event of Ionian islands (Greece), *Geophys. J. Int.*, **105,** 529–535.

Kiratzi, A. A., Wagner, G. S. & Langston, Ch. A., 1991. Source parameters of some large earthquakes in northern Aegean determined by body waveform inversion, *Pure appl. Geophys.*, **135,** 515–527.

Kissel, C. & Laj, C., 1988. The tertiary geodynamical evolution of the Aegean arc; a paleomagnetic reconstruction, *Tectonophysics,* **146,** 183–201.

Kissel, C., Laj, C. & Mazaud, A., 1986. Paleomagnetic results from Neogene formations in Evia, Skyros, and the Volos region and the deformation of Central Aegea, *Geophys. Res. Lett.*, **13,** 1446–1449.

Kovachev, S. A., Kuzin, I. P. & Soloviev, S. L., 1992. Microseismicity of the frontal Hellenic arc according to OBS observations, *Tectonophysics,* **201,** 317–327.

Laj, C., Jamet, M., Sorel, D. & Valente, J. P., 1982. First paleomagnetic results from Mio–Pliocene series of the Hellenic sedimentary arc, *Tectonophysics,* **86,** 45–67.

Lêîté, O. Mascle, J. & Anastasakis, G., 1980. La marge continentale sudcrétoise: grands ensembles structuraux et sédimentaires, *C.R. Somm. Séances Soc. Géol. France,* **5,** 171–174.

Le Pichon, X. & Angelier J., 1979. The Hellenic arc and trench system: a key to the neotectonic evolution of the Eastern Mediterranean region, *Tectonophysics,* **60,** 1–42.

Le Pichon *et al.*, 1981. Active tectonics in the Hellenic trench, *Oceanologica Acta,* Special Issue, 273–281.

Le Pichon, X., Lyberis, N., Angelier, J. & Renard, V., 1982. Strain distribution over the east Mediterranean ridge: a synthesis incorporating new Sea-Beam data, *Tectonophysics,* **86,** 243–274.

Le Quellec, P., Mascle, J., Got, H. & Vittori, J., 1980. Seismic structure of southwestern Peloponnesus continental margin, *Am. Assoc. Petrol. Geol. Bull.*, **64,** 242–263.

Liakopoulou, F., Pearce, R. G. & Main, I. G., 1991. Source mechanisms of recent earthquakes in the Hellenic arc from broadband data, *Tectonophysics,* **200,** 233–248.

Lyberis, N., Angelier, J., Barrier, E. & Lallemant, S., 1982. Active deformation of a segment of arc: the strait of Kythira, Hellenic arc, Greece, *J. struct. Geol.*, **4,** 299–312.

Lyon-Caen, H. *et al.*, 1988. The 1986 Kalamata (South Peloponnesus) earthquake: Detailed study of a normal fault, evidences for east–west extension in the Hellenic Arc, *J. geophys. Res.*, **93,** 14 967–15 000.

Makris, J. & Stobbe, C., 1984. Physical properties and state of the crust and upper mantle of the Eastern Mediterranean sea deduced from geophysical data, *Mar. Geol.*, **55,** 347–363.

Makroupoulos, K. & Burton, P. W., 1984. Greek tectonics and seismicity, *Tectonophysics,* **106,** 275–304.

Martin, Ch., 1988. Géométrie et cinématique de la subduction égéenne, structure en vitesse et atténuation sous le Péloponnèse, *Thèse,* Université Joseph Fourier, Grenoble.

Mascle, J. & Martin, L., 1990. Shallow structure and recent evolution of the Aegean Sea: A synthesis based on continuous reflection profiles, *Mar. Geol.*, **94,** 271–299.

Mascle, J., Jongsma, D., Campredon, R., Dercourt, J., Glaçon, G., Lecleach, A., Lybéris, N., Malod, J. A. & Mitropoulos, D., 1982. The Hellenic margin from eastern Crete to Rhodes: preliminary results, *Tectonophysics,* **86,** 113–132.

Mascle, J., Le Cleac'h, A. & Jongsma, D., 1986. The eastern Hellenic Margin from Crete to Rhodes: Example of progressive collision, *Mar. Geol.*, **73,** 145–168.

McKenzie, D. P., 1972. Active tectonics of the Mediterranean region, *Geophys. J. R. astr. Soc.*, **30,** 109–185.

McKenzie, D. P., 1978. Active tectonics of the Alpine–Himalayan belt: the Aegean Sea and surrounding regions, *Geophys. J. R. astr. Soc.*, **55,** 217–254.

Mercier, J. L., 1981. Extensional–compressional tectonics associated with the Aegean Arc: comparison with the Andean Cordillera of south Peru–North Bolivia, *Phil. Trans. R. Soc. Lond.*, **300,** 337–355.

Mercier, J. L., Carey, E., Philip, H. & Sorel, D., 1976. La néotectonique plio-quaternaire de l'arc égéen externe et de la mer Egée et ses relations avec la sismicité, *Bull. Soc. Géol. France,* **7,** 355–372.

Mercier, J. L., Delibasis, N., Gautier, A., Jarrige, J. J., Lemeille, F., Philip, H., Sébrier, M. & Sorel, D., 1979. La néotectonique de l'Arc Egéen, *Rev. Géol. Dyn. Géogr. Phys.*, **21,** 67–92.

Mercier, J. L., Sorel, D., Vergely, P. & Simeakis, K., 1989. Extensional tectonic regimes in the Aegean basins during the Cenozoic, *Basin Res.*, **2,** 49–71.

Merle, O., 1989. Strain models within spreading nappes, *Tectonophysics,* **165,** 57–71.

Morelli, C., Pisani, M. & Gantar, C., 1975. Geophysical studies in the Aegean Sea and in the Eastern Mediterranean, *Boll. Geofis. Teor. Appl.*, **18,** 127–167.

Ouyed, M., Yielding, G. Hatzfeld, D. & King, G. C. P., 1983. An aftershock study of the El Asnam (Algeria) earthquake of 1980 October 10, *Geophys. J. R. astr. Soc.*, **73,** 605–639.

Papadopoulos, T., Wyss, M. & Schmerge, D. L., 1988. Earthquake locations in the Western Hellenic arc relative to the plate boundary, *Bull. seism. Soc. Am.*, **78,** 1222–1231.

Papazachos, B. C. & Comninakis, P. E., 1971. Geophysical and tectonic features of the Aegean arc, *J. geophys. Res.*, **76,** 8517–8533.

Papazachos, B. C. & Comninakis, P. E., 1982. Long term earthquake prediction in the Hellenic trench arc system, *Tectonophysics,* **86,** 3–16.

Papazachos, B. & Papazachos, K., 1989. *Earthquakes in Greece,* Ekdoseis Ziti, Thessaloniki.

Papazachos, B. C., Kiratzi, A. A., Karacostas, B., Panagiotopoulos, D., Scordilis, E. & Mountrakis, D. M., 1988. Surface fault traces, fault plane solution and spatial distribution of the aftershocks of September 13, 1986 earthquake of Kalamata (Southern Greece), *Pure appl. Geophys.*, **126,** 55–68.

Reasenberg, P. A. & Oppenheimer, D., 1985. FPFIT, FPPLOT, FPPAGE: Fortran computer programs for calculating and displaying earthquake fault-plane solutions, *USGS Open File Report No.* 85–739.

Ritsema, A. R., 1974. Earthquakes mechanisms of the Balkan region, *UNDP/UNESCO report on Survey of the Seismicity of the Balkan Region, project REM/70/172.*

Sonder, L. & England, P., 1989. Effects of a temperature-dependant rheology on large-scale continental extension, *J. geophys. Res.*, **94,** 7603–7619.

Speranza, F., Kissel, C., Islami, I., Hyseni, A. & Laj, C., 1992. First palaeomagnetic evidence for rotation of the Ionian zone of Albania, *Geophys. Res. Lett.*, **19,** 697–700.

Taymaz, T., Jackson, J. A. & Westaway, R., 1990. Earthquake mechanisms in the Hellenic Trench near Crete, *Geophys. J. Int.*, **102,** 695–732.

Taymaz, T., Jackson, J. A. & McKenzie, D., 1991. Active tectonics of the north and central Aegean Sea, *Geophys. J. Int.*, **106,** 433–490.

Truffert, C., Chamot-Rooke, N., Lallemant, S., De Voogd, B., Huchon, P. & Le Pichon, X., 1993. The crust of the Western Mediterranean Ridge from deep seismic data and gravity modelling, *Geophys. J. Int.*, **114,** 360–372.

Wyss, M. & Baer, M., 1981. Earthquake hazard in the Hellenic arc, in *Earthquakes Prediction*, M. Ewing Series, Am. geophys. Un. 4, 53–172.

APPENDIX: LOWER HEMISPHERE OF FOCAL SPHERES OF CRUSTAL EARTHQUAKES

Solid and open symbols are reliable compressional and dilatational first motions; + and − are uncertain.

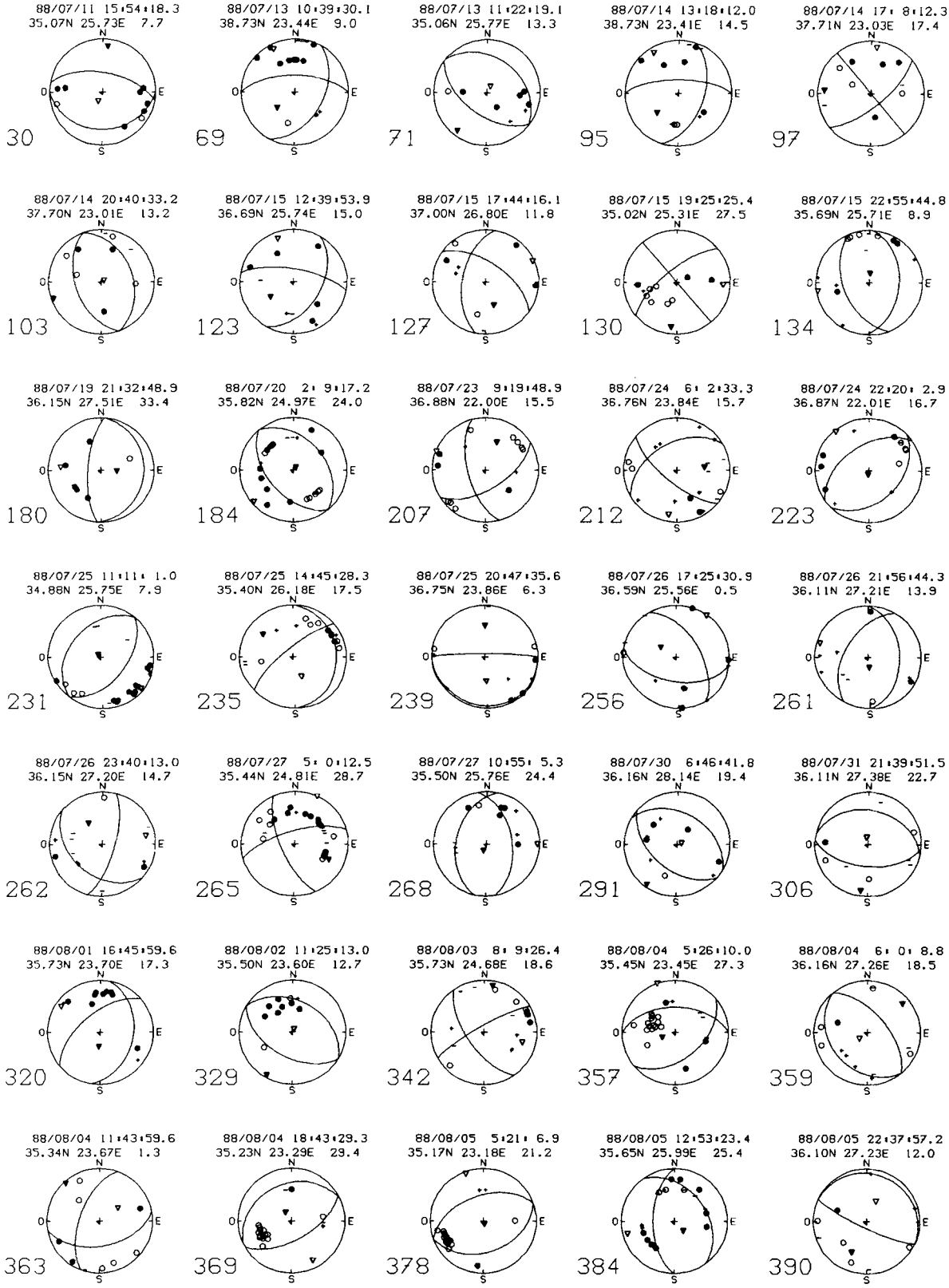

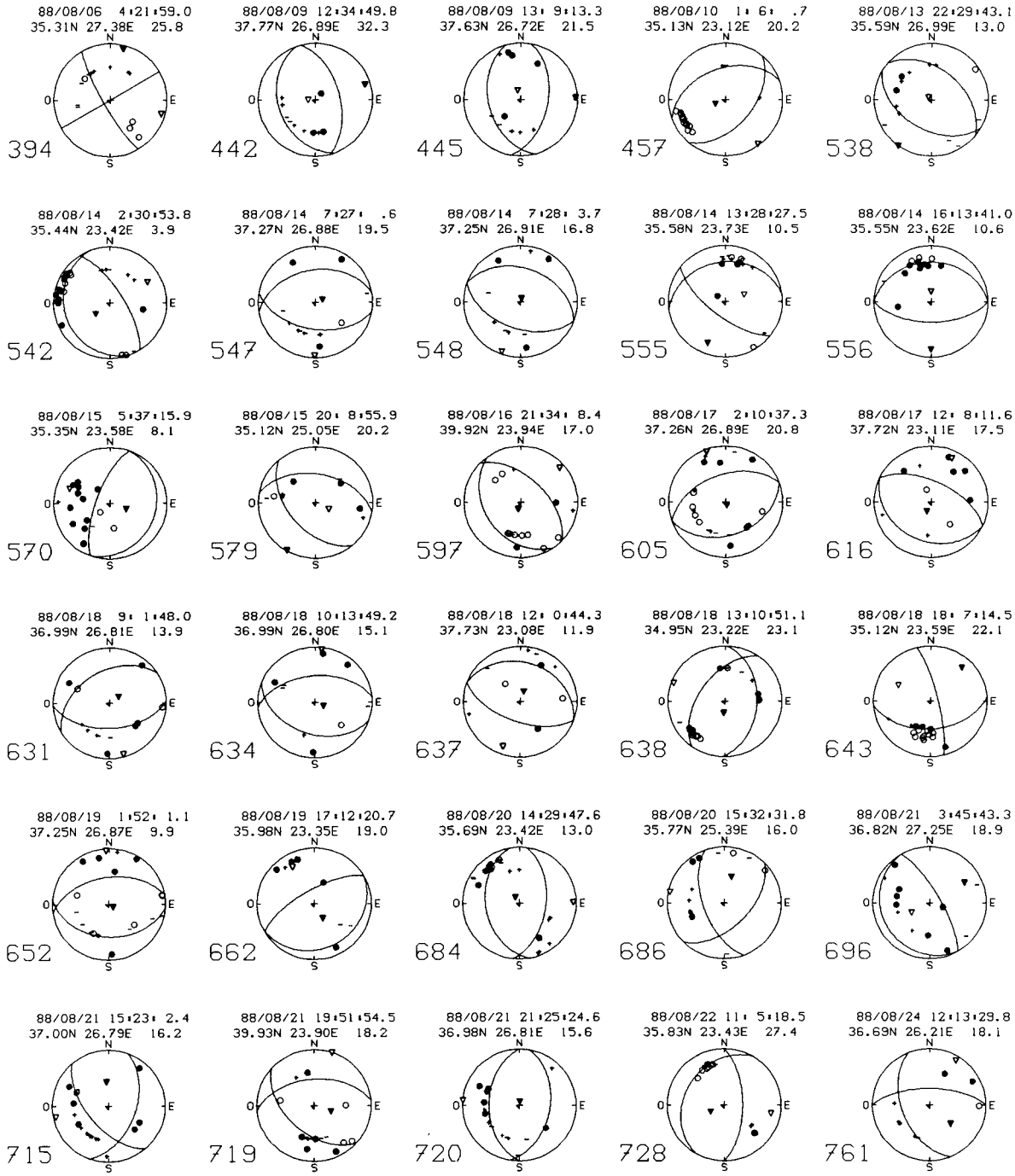
88/08/06 4:21:59.0
35.31N 27.38E 25.8
394
88/08/09 12:34:49.8
37.77N 26.89E 32.3
442
88/08/09 13: 9:13.3
37.63N 26.72E 21.5
445
88/08/10 1: 6: .7
35.13N 23.12E 20.2
457
88/08/13 22:29:43.1
35.59N 26.99E 13.0
538
88/08/14 2:30:53.8
35.44N 23.42E 3.9
542
88/08/14 7:27: .6
37.27N 26.88E 19.5
547
88/08/14 7:28: 3.7
37.25N 26.91E 16.8
548
88/08/14 13:28:27.5
35.58N 23.73E 10.5
555
88/08/14 16:13:41.0
35.55N 23.62E 10.6
556
88/08/15 5:37:15.9
35.35N 23.58E 8.1
570
88/08/15 20: 8:55.9
35.12N 25.05E 20.2
579
88/08/16 21:34: 8.4
39.92N 23.94E 17.0
597
88/08/17 2:10:37.3
37.26N 26.89E 20.8
605
88/08/17 12: 8:11.6
37.72N 23.11E 17.5
616
88/08/18 9: 1:48.0
36.99N 26.81E 13.9
631
88/08/18 10:13:49.2
36.99N 26.80E 15.1
634
88/08/18 12: 0:44.3
37.73N 23.08E 11.9
637
88/08/18 13:10:51.1
34.95N 23.22E 23.1
638
88/08/18 18: 7:14.5
35.12N 23.59E 22.1
643
88/08/19 1:52: 1.1
37.25N 26.87E 9.9
652
88/08/19 17:12:20.7
35.98N 23.35E 19.0
662
88/08/20 14:29:47.6
35.69N 23.42E 13.0
684
88/08/20 15:32:31.8
35.77N 25.39E 16.0
686
88/08/21 3:45:43.3
36.82N 27.25E 18.9
696
88/08/21 15:23: 2.4
37.00N 26.79E 16.2
715
88/08/21 19:51:54.5
39.93N 23.90E 18.2
719
88/08/21 21:25:24.6
36.98N 26.81E 15.6
720
88/08/22 11: 5:18.5
35.83N 23.43E 27.4
728
88/08/24 12:13:29.8
36.69N 26.21E 18.1
761